NASA TECHNICAL MEMORANDUM 100628

FATIGUE TESTING AND DAMAGE DEVELOPMENT IN CONTINUOUS FIBER REINFORCED METAL MATRIX COMPOSITES

W. S. Johnson

JUNE 1988

NASA
National Aeronautics and
Space Administration

Langley Research Center
Hampton, Virginia 23665-5225

FATIGUE TESTING AND DAMAGE DEVELOPMENT IN CONTINUOUS FIBER REINFORCED METAL MATRIX COMPOSITES

W. S. Johnson
Senior Research Engineer
NASA Langley Research Center
Hampton, Virginia

SUMMARY

Continuous fiber reinforced metal matrix composites (MMC) are projected for use in high temperature, stiffness critical parts that will be subjected to cyclic loadings. This paper presents a general overview of the fatigue behavior of MMC. The objectives of this paper are twofold. The first objective is to present experimental procedures and techniques for conducting a meaningful fatigue test to detect and quantify fatigue damage in MMC. These techniques include interpretation of stress-strain responses, acid etching of the matrix, edge replicas of the specimen under load, radiography, and micrographs of the failure surfaces. In addition, the paper will show how stiffness loss in continuous fiber reinforced metal matrix composites can be a useful parameter for detecting fatigue damage initiation and accumulation. Second, numerous examples of how fatigue damage can initiate and grow in various MMC are given. Depending on the relative fatigue behavior of the fiber and matrix, and the interface properties, the failure modes of MMC can be grouped into four categories: (1.) matrix dominated, (2.) fiber dominated, (3.) self-similar damage growth, and (4.) fiber/matrix interfacial failures. These four types of damage will be discussed and illustrated by examples with the emphasis on the fatigue of unnotched laminates.

INTRODUCTION

Fatigue of metal matrix composites can be quite complex. The matrix, because of its relatively high strength and stiffness compared to the fiber, plays a very active role compared to a polymer matrix. Fatigue damage in a metal matrix can reduce the laminate stiffness by as much as 50% without causing laminate failure [1]. This paper will describe various experimental approaches to quantifying fatigue damage, and will discuss a number of examples of damage development and failure along with some associated analytical models of MMC behavior.

Stiffness loss in continuous fiber reinforced metal matrix composites has been a useful parameter for detecting fatigue damage initiation and accumulation [1-5]. Specific aspects of measuring and interpreting the stiffness loss will be covered. Various techniques for defining the fatigue damage will be presented. These techniques include acid etching of the matrix, edge replicas, radiography, and micrographs of the failure surfaces.

The fatigue failure modes in continuous fiber reinforced metal matrix composites are controlled by the fiber and matrix and by the fiber/matrix interface. The relative strains to fatigue failure of the fiber and matrix will determine the failure mode provided the fiber/matrix interface is strong enough to support the required load. If the matrix requires much less cyclic strain to fatigue than the fiber, then the matrix damage will dominate. If, on the other hand, the fiber requires less cyclic strain to fail than does the matrix, the fiber damage will dominate. This composite will fail rather suddenly in fatigue with little warning, provided the fiber/matrix interface is strong enough to transfer load into the broken fibers. The fiber/matrix interface may be unable to carry the required stress and may fail, causing fiber/matrix separation. This is likely to occur in those MMC systems with high yield strength matrices that cause high load transfer between fiber and matrix in the off-axis plies. Lastly, if both the fiber and matrix require approximately the same cyclic strain for fatigue failure and the fiber/matrix interface is sufficiently strong, self-similar crack growth, as found in metals, may result. Self-similar crack growth is also possible when the matrix is strong enough to create a high stress concentration in the fiber ahead of the matrix crack. Thus, by starting the fatigue damage in the matrix, the crack can propagate across the fibers.

As new continuous fiber-reinforced metal matrix composites are hypothesized and developed, projections of their fatigue behavior can be made by understanding the relative strengths of the fiber, matrix, and the fiber/matrix interface. This paper is intended to be a guide that might be considered when planning a program to furnish some insight into what type of fatigue damage may occur and how the damage might be quantified.

EXPERIMENTAL TECHNIQUES

This section will describe some experimental techniques that the author has used over the years to detect and quantify fatigue damage in a variety of continuous fiber reinforced MMC. First, the discussion will address the recorded stress-strain response of the material. Several different moduli can be measured from the recorded stress-strain response to can aid in the understanding of fatigue damage development. The remainder of this section will address several experimental techniques that have been found useful for quantifying damage in MMC.

Stress-Strain Data Reduction

Strain gages are commonly used to measure the specimens strain response. However, strain gages only measure local strains. In general, fatigue damage in unnotched composite laminates may be quite random. Unless the strain gage is quite large, the local strain measured may or may not reflect the random damage. O'Brien [6] has discussed the effect of gage-section size on composite stiffness measurements. The author suggests the use of an extensometer to measure the strain over a 25.4 mm (1.0 inch) gage section. This will result in a global measurement on the effect of damage on the laminate moduli.

The cyclic stress-strain response as presented in Figure 1 can be analyzed to yield several mechanical properties of a metal matrix composite laminate. These properties include:

Initial elastic modulus (tangent modulus)
Stiffness (secant modulus)
Permanent plastic deformation (strain)
Elastic unloading modulus after N number of cycles
Stiffness after N number of cycles
Cyclic strain
Number of cycles to fatigue failure
Strain to static failure
Residual strength after a set number of cycles.

A detailed definition of each property along with the physical significance is presented next.

Initial elastic modulus: The elastic modulus, E, is the tangent modulus of the initial linear portion of the loading curve. The initial elastic modulus, E_I, is measured on the first loading cycle as shown in Fig. 1. E_I can be compared to the analytically predicted lamination theory elastic modulus for an undamaged composite. The initial elastic modulus is significant in that all later measurements of elastic modulus at N cycles will be compared to this initial modulus to give an indication of the amount of fatigue damage accumulated by the composite laminate.

Stiffness: The stiffness, E_S, is essentially the secant modulus of the loading cycle as indicated in Fig. 2. In order to eliminate permanent plastic deformation from the stiffness measurement, the stiffness is defined utilizing the unloading portion of the cycle (the stress range, ΔS, divided by the unloading strain range, $\Delta\epsilon$). The initial stiffness can be compared to measurements of stiffness at N cycles and is therefore significant.

The stiffness may be a useful measurement to design engineers since this is the total strain of the material in response to an applied load. (This is after no additional permanent plastic strain occurs during cyclic loading.) The stiffness is a combination of the elastic properties of the laminate as well as the plastic behavior of the metal matrix. The stiffness is, therefore, a function of the matrix yield stress. As will be shown subsequently, the matrix may cyclically harden and the stiffness increase during the time damage initiates. However, as the fatigue damage in the laminate grows, the stiffness decreases. Therefore, cannot determine the onset and extent of fatigue damage in a metal matrix composite using a stiffness (secant modulus) criterion alone.

Permanent plastic strain: The permanent plastic strain, ϵ_p, is measured directly from the stress-strain curve. The permanent strain is usually accumulated in the first three or four cycles with little additional permanent strain accumulating thereafter. The accumulated permanent strain gives a good indication of the amount of residual stress in the 0^o fibers since all the constituents in the composite are assumed to strain the same.

Elastic unloading modulus after N number of cycles: The elastic unloading modulus E_N is measured directly from the stress-strain curve at intervals throughout the life of the composite. See Fig. 2. The percentage of the elastic unloading modulus at N cycles, E_N, as divided by the initial elastic modulus,

$$E_N/E_I \times 100 = \% E_I$$

can be plotted against the number of fatigue cycles, N, in order to present fatigue damage as a function of constant amplitude cycling at a prescribed stress ratio and maximum stress.

Stiffness after N number of cycles: The stiffness (secant modulus) is measured as the stress range divided by the unloading strain range. The percentage of the initial stiffness is calculated by dividing the stiffness at N cycles, E_{NS}, by the initial stiffness, E_{IS},

$$E_{NS}/E_{IS} \times 100 = \% E_{IS}.$$

The $\% E_{IS}$ can be plotted against the number of fatigue cycles, N, in order to compare a "stiffness" and "elastic modulus" criteria

for assessing fatigue damage.

Cyclic strain: The cyclic strain, $\Delta\epsilon$, is measured directly from the stress-strain curve. The cyclic strain is a direct indicator of the cyclic stress in the 0^o fibers. The $\Delta\epsilon$ can be used to examine the possible correlation between the composite strain and fatigue endurance. The cyclic strain can also be multiplied by the elastic fiber modulus to calculate the cyclic fiber stress in the 0^o plies.

Number of cycles to fatigue failure: The number of cycles to fatigue failure, N_F, plotted against the maximum cyclic stresses for a given value of stress ratio is the traditional S-N curve. This type of data indicates the maximum cyclic stress (referred to as the fatigue endurance limit) at a given stress ratio that the composite laminate can be expected to survive ($2x10^6$ cycles for example). The S-N curve does not, however, indicate the physical condition of the laminate at the established endurance limit other than the fact that the laminate can survive the endurance stress.

Residual static strength: Fatigue specimens that survive $2x10^6$ cycles without failure, can be tested for residual strength to correlate fatigue damage and residual strength. The stress at failure, which is the maximum stress from the stress-strain curve, is defined as the residual static stress, S_F.

Strain to static failure: For static strength tests, unfatigued composite specimens are loaded to failure. Thus, the strain to static failure, ϵ_{ftot}, is measured from zero stress to the maximum static stress. The ϵ_{ftot} is used to estimate the 0^o fiber ultimate stress.

Matrix Etching

After a specimen has been statically or fatigue loaded, matrix etching can be used to reveal two types of composite damage. First, etching away the matrix material will expose the fibers. The fibers can then be inspected for breaks. Secondly, by carefully etching away the matrix in the outer ply and then removing the exposed fibers, the next layer can be examined for matrix cracking and fiber damage. This technique can be used to systematically examine the damage of each ply in a laminate.

For 6061 aluminum matrix composites, a 30% HCL solution in distilled water was found to be effective for etching away the matrix without detectable damage to either boron or silicon-carbide fibers. The actual etching process must be carefully controlled if one wishes to remove one layer at a time to inspect the matrix in the underlying layers. Enough matrix material must be etched away to allow the surface layer of fibers to be removed; however, if too much matrix material is removed, the matrix damage in the underlying

ply will not be observable because the matrix has been etched away. This process is a trial and error operation at best and will probably require several attempts before a satisfactory result is obtained.

Edge Replica Technique

In the edge replica technique, a permanent impression of the specimen edge is produced in a cellulose acetate film. The advantage of this technique is that the replica can be taken while the specimen is under load in the test machine. The replica can then be examined later for details of damage, such as matrix cracks, split fibers, or fiber/matrix seperations. This technique can be easily used for replicating any surface for microstructural detail.

Essentially a softened acetate film is held against the desired surface to be replicated. Acetone is applied to face of the film to soften it. The acetone serves to polymerize the acetate, making it viscous enough so as to flow into the micro-structural cavities present on the surface. Pressure is applied to the back side of the film to aid in the flow process. The acetate film is allowed to dry in place for 3-5 minutes and then is carefully peeled from the surface. The replica can now be sputtered with gold (a thin layer of Au-Pd alloy) and viewed in a scanning electron microscope (SEM).

Radiography

In some fiber/matrix combinations, radiography can be a very helpful tool for monitoring fiber failures. The tungsten core found in boron fibers shows very clearly in the radiograph. Fiber breaks appear as gaps in the tungsten core. On the other hand, silicon-carbide fibers with graphite cores are not visible in radiographs. Basically, the greater the difference between the mass density of the fiber and the matrix, the better is the resolution of the individual fiber. Portable X-ray units are available that can be used to radiograph specimens while under load in the test stand.

Acoustic Emissions

When a fiber fails or the matrix cracks, energy is released in a fashion such that an acoustic wave is emitted. Acoustic emission (AE) transducers can receive these signals and record their intensities. Through systematic experimental observation of damage development and correlation with acoustic emissions signals, a damage development quantification scheme can be developed based on recorded acoustic emissions. The author has used acoustic emissions to monitor fiber breaks at notch tips in boron/aluminum laminates [7] under static loading. In addition, Awerbuch [8] has used AE techniques extensively to monitor damage accumulation in MMC;

therefore, ref. 8 should be consulted for further details on the applicability of this technique.

Micrographs

Fracture surfaces and interface characteristics can be examined using scanning electron microscope (SEM) and energy dispersive X-ray analysis (EDAX). A SEM can be used to distinguish fatigue striation markings from dimple fracture patterns in order to determine if a portion of the fracture surface failed due to fatigue or static fracture. The SEM is also very useful for close-up viewing of any type of micro-structural damage. The EDAX is useful for the determination of the chemical composition of the failure surface. This is specifically useful for determining whether the failure occurred in the fiber, matrix, or in some reaction zone between the fiber and the matrix.

The author has also had considerable success documenting damage, such as matrix cracking, by taking photographs through a 30-60 power optical microscope.

OBSERVATIONS OF FAILURE MODES

This section will review various fatigue failure modes that have been reported in the literature for continuous fiber reinforced metal matrix composites. Metal matrix composites consist of high strength - high stiffness fibers embedded in a metal matrix. In typical polymer matrix composites, the moduli of the fibers are always much higher than those of the polymer matrix material, perhaps two orders of magnitude higher. In contrast, the metal matrix may have a modulus of the same order of magnitude as the fiber. One reason MMC are attractive materials is their high stiffness to weight ratio. For a cyclic stress level well below that required to fail the laminate, fatigue damage may cause significant stiffness loss in the laminate. The understanding of the damage mechanisms that could cause loss of laminate stiffness is just as important as understanding the final failure mechanisms.

The difference between the ultimate strain of the fiber and the matrix may play a big role in determining where fatigue damage initiates and how it grows under static loading. Based on the difference between strains to fatigue failure of the fiber and matrix, the possible failure modes of MMC can be grouped into three categories: (1.) matrix dominated, (2.) fiber dominated, and (3.) self-similar damage growth. A fourth type of damage development is dependent on the relative strength of the fiber/matrix interface, (4.) fiber/matrix interfacial failures. These four types of damage will be discussed and illustrated by examples in the remainder of the paper.

Matrix Dominated Damage

In boron/aluminum composites, the boron fibers are very fatigue insensitive. They are rather large diameter (0.14 mm) fibers, with very smooth sides, and are virtually elastic until fracture. Boron has a strain to failure of about 0.0085. While the strain to failure of 6061-0 aluminum is almost 0.1, it yields at a strain between 0.001 and 0.002. Therefore, under static loading the fibers reach their critical strain first and fail before the matrix [7]. But under fatigue loading, the matrix cyclically yields at strain levels far below critical strains for the fibers. This cyclic yielding results in fatigue damage to the matrix but not to the fibers. Therefore in this material, fatigue damage is matrix dominated.

First, let us examine why fatigue cracks would develop in the matrix material at such a low strain. If fatigue damage in general is to be avoided, and low cycle fatigue failures in particular, the cyclic loading must produce only elastic strains in the constituents. Even so, local plastic straining can be permitted in the composite during the first few load cycles, provided that the composite "shakes down" during these few cycles. The shakedown stress is reached if the matrix cyclically hardens to a yield stress, Y, such that, subsequently, only elastic deformation occurs under load cycles [2]. Previous tests have shown that the matrix fatigue limit coincides with the stable cyclic yield stress for annealed aluminum [11,12] and steels [12]. The value of Y is 70.38 MPa for annealed 6061 aluminum [1].

The possible relationship between fatigue and shakedown in metal matrix composites was first suggested by Dvorak and Tarn [9] in 1975 and related to then available experimental data, obtained primarily for unidirectional 6061 B/Al materials. Dvorak and Tarn suggested that the shakedown stress was related to laminate S-N type fatigue failure. Since 1979 Dvorak and Johnson [2,3,10], have examined theoretically and experimentally both unidirectional and laminated 6061-0 B/Al composites. They found that the shakedown stress was related to the onset of fatigue damage in the composite's matrix material but not necessarily to laminate failure.

The shakedown stress range for a unidirectionally loaded laminate can be found by using laminate theory to determine the yield surface for individual plies in a laminate. Figure 3 shows an example of a $[0/\pm45/90/0/\pm45/90]_s$ lay-up under biaxial inplane stresses S_{11} and S_{22} [1]. Each ply has its own elliptical yield surface, constructed analytically from ply matrix stresses and the von Mises yield condition. The overall yield surface of the laminate is an internal envelope of the yield surfaces of individual plies. The shakedown stress range, ΔS_{Sh}, is the width of the overall yield surface in the S_{11} direction for uniaxial loading. The value of ΔS_{Sh} can b e calculated easily with the computer

program AGLPLY [13]. The program essentially uses lamination theory, the von Mises yield criteria, and the vanishing fiber diameter material model to calculate the elastic-plastic laminate response. The shakedown range is approximately twice the minimum laminate stress for first yielding [2].

Laminates containing 0^o plies

Next, several examples will be given of the type of fatigue damage that occurs in B/Al and SCS_6/Al composites that contain 0^o plies when subjected to cyclic loadings above their respective shakedown range. Figure 4 presents the fatigue damage accumulation as a function of number of applied cycles and stress for a $[0/\pm45\pm/90/0/\pm45/90]_s$ laminate [3]. The damage is expressed in terms of E_N/E_I, the percent of the initial elastic unloading modulus remaining after N number of cycles. After 2,000,000 cycles, the tests were terminated. Notice that each specimen appears to reach a stabilized value of E_N/E_I, herein referred to as a "saturation damage state" (SDS). All of the specimens shown in Fig. 4 were cyclically loaded below the laminate's 375 MPa fatigue limit. S-N data and the associated fatigue limits are presented in Ref 1 for six different laminates. The SDS implies that the laminate will neither accumulate more damage nor fail under the present loading condition.

Figure 5 presents the SDS as a function of stress range by plotting the values after 2,000,000 cycles. This figure includes data for R=0.1 and 0.3. The constant amplitude SDS is a function of stress range and is independent of mean stress. The data can be extrapolated, using a regression analysis, to 100 percent of E_N/E_0 (that is, no change in elastic unloading modulus) to determine the stress range below which no fatigue damage accumulates. Very good agreement was found between this no damage stress range and the predicted shakedown range [3].

Figure 6 is a plot of the percent of initial stiffness and the percentage of initial elastic unloading modulus versus the number of cycles [1]. Notice that the stiffness actually increases over the first portion of the fatigue life to a point at 100,000 cycles where it is approximately 5 percent greater than the initial value. This stiffness increase is due to a cyclic hardening of the matrix material that raises the yield strength. The initial elastic unloading modulus data is constant up to 10,000 cycles then the modulus begins to decrease, indicating fatigue damage in the composite. This type of behavior has been found to be common for other laminates of B/Al and SCS_2/Al composites containing off-axis plies. Clearly the initial elastic unloading modulus is a better indicator of the initiation of fatigue damage while the stiffness is a better descriptor of the overall stress-strain response of the laminate.

Etching away the matrix materials and exposing the fibers revealed that essentially no 0^o fiber broke unless the specimen was fatigue loaded to within 10 percent of the fatigue limit load. The drop in the elastic unloading modulus of those specimens cycled at stress levels below the fatigue limit can be attributed almost entirely to cracking in the matrix material between the fibers in the off-axis plies. Several micrographs of this cracking will be discussed next.

Figure 7 shows the matrix cracking in the 45^o layer, just beneath the 0^o ply of a boron/aluminum laminate [3]. The cracks grow parallel to the fiber direction. Figure 8a shows part of a fatigue failure surface of a specimen that failed at 33,170 cycles. The close-up in Fig. 8b is of the matrix material between the 45^o and -45^o plies. One can actually see the crisscross pattern of the matrix cracks from each ply. Figure 9 shows the same sort of matrix cracking in the 90^o ply. In Figs. 7 and 9 the matrix cracks shown were in the ply just beneath the 0^o surface ply. In neither case did the matrix cracks grow past the 0^o fibers to the surface of the specimen. Apparently, such a layer of fibers is very effective at restricting crack growth past the layer of fibers in any direction other than parallel to the fiber direction. Also, the effective stress in the 0^o layer matrix material is lower than that found in the off-axis plies, thus cracks are less likely to grow in the 0^o layer. A SEM micrograph is presented in Fig. 10 to show the fatigue striations in one of the matrix cracks [1]. Fig. 10 is proof that the cracks are a product of fatigue crack initiation and growth.

The author has formulated a rather simple model that predicts the effect of the matrix cracking on laminate stiffness [4,5]. This model has been verified for a variety of different lay-ups of boron/aluminum and silicon-carbide/aluminum composites. The model is briefly reviewed in the Appendix. A more sophisticated, rigorous approach has been suggested [15] to account for the actual stiffness reduction due to the individual matrix cracks. However this approach is very complex and the results are similar to those found for the simple model.

Laminates with no 0^o plies

The $[\pm 45]_{2s}$ SCS_2/Al laminate data [5] presented in Fig. 11 is unique among the laminates tested since it has no 0^o fibers to pick-up the load from the damaged matrix. (The cross sectional area actually decreases some what during the cyclic loading. The stress is calculated based on the initial area, as has been all other calculations of stress reported herein, and is plotted in Fig. 11 as the engineering stress.) Below the shakedown stress range of 150 MPa, shown in Fig 11, the specimen underwent large plastic deformations (as much as 0.08 strain). Also, during cyclic loading, the matrix yield stress changed from its initial value of 40 MPa to a fully hardened, stabilized value of 150 MPa. The rotation of fibers (to approximately $\pm 41^o$) actually caused the elastic modulus

and secant modulus to increase slightly. The cross-sectional area of the specimen decreased by approximately 8% during a cyclic stress range of 138 MPa. Below the shakedown stress range, the stress-strain behavior of the laminate stabilized and no fatigue damage was noticed.

Above the shakedown stress range, fatigue damage developed in the $[\pm 45]_{2s}$ laminate in the form of many matrix cracks growing into the specimen from the edge. Under these conditions, the elastic modulus and the secant modulus of the laminate decreased. At S=172 MPa the fibers rotated to $\pm 39^{o}$. Once fatigue damage initiated in the matrix it eventually grew to cause laminate failure since there were no 0^{o} fibers to carry the load in a strain controlled fashion. Thus, the fatigue limit of laminates containing no 0^{o} fibers may be estimated by the shakedown stress range.

Laminates Containing Holes or Slits

Grimsley [16] used the previously discussed shakedown model along with a stress analysis of a pin loaded hole joint to predict the loads at which joint specimens would fail in fatigue. Failure was defined as a 1.27 mm elongation of the hole as measured by the pin deflection. Specimens were made of B/Al, SiC/Al, and B_4C/Al (borsic fiber reinforced aluminum). One joint specimen, for which the stress at the edge of the hole was below the shakedown stress, did not fail after five million constant amplitude fatigue cycles. Other joint specimens were fatigued above the calculated shakedown limit at the edge of the hole and failed within a half million cycles. This limited amount of data supports the use of the shakedown theory for predicting local damage around notches.

Harmon, Saff, and Sun [17] has additional data to support this approach for aluminum matrix composites with holes. Figure 12 shows both fiber and matrix fatigue failure modes for an unidirectional B/Al specimen containing a filled hole. Note that when the stress level is too low to cause matrix yielding (less than 30% ultimate tensile strength), the lives to crack initiation (represented by a 1.27 mm long crack) are very long. As the load levels increase, lives to crack initiation decrease but the fiber stresses will not cause failure. At load levels above approximately 75 percent of the ultimate, fiber failure begins to control the life. Fiber failures can occur at such short lives (stress above 80%) that matrix cracks will not develop before failure.

Ref. 17 also reported that when notched unidirectional B/Al specimens are fatigued at stress levels above matrix yield but below fiber failure, cracks initiated in the matrix at the notch tip and grew parallel to the fibers. These cracks were driven by shear in the matrix. This matrix shear stress was a constant driver since the flaw growth did not affect the net section or other geometrical parameter. This constant driving force was reflected by nearly constant crack growth rates measured experimentally.

Simonds [18] fatigued several different B/Al laminates containing centered crack-like slits. The fatigue load was high enough to cause damage at the end of the slit but low enough not to cause laminate failure in 100,000 cycles. Some specimens were radiographed and others were sectioned and examined microscopically to determine the extent of fatigue damage in terms of fiber failures and matrix cracking. Many split or broken 45^{o} fibers were found at the slit tip. This reflects the low transverse strengths of the boron fibers as reported by Johnson, Bigelow, and Bahei-El-Din [7] and Johnson [3]. Considerable matrix cracking was found in the 45^{o} plies at the slit tip. In those specimens containing at least 50% 0^{o} plies, matrix cracks in the 0^{o} direction were found at the slit tip growing parallel to the fibers toward the grips. Since the fatigue levels chosen ranged from 25 to 50% of the static ultimate stress for the unidirectional specimens and from 50 to 80% for those specimens with cross plies, broken 0^{o} fibers were seldom found at the slit tip. Therefore, the fatigue damage had a negligible effect on the residual static strength which is primarily a function of the 0^{o} fibers.

Summary of Matrix Dominated Damage

Matrix damage can affect the laminate stiffness properties significantly. For unnotched specimens, the resulting secant modulus after 500,000 cycles is significantly below the elastic modulus for all of the tested laminates, except the $[0]_8$ laminates. If compared at a cyclic strain range of 0.004, the $[0]_8$ laminate retained approximately 95% of the original elastic modulus. The other laminates retained about 60 to 70% of their original moduli. These differences between the often calculated elastic modulus and the resulting secant modulus must be addressed by the designers of stiffness critical parts. Certainly, the unidirectional laminate may still retain the desired stiffness, but laminates with off-axis plies must be scrutinized for their design load levels and stiffness requirements.

The results presented for matrix dominated fatigue damage indicate the existence of three distinct regions in the S-N plane in which one observes different responses of MMC to cyclic loading. Figure 13 illustrates these regions for a $[0/\pm45/90/0/\pm45/90]_s$ B/Al laminate. At low stress levels, below the shakedown stress limit (218 MPa), there is no significant fatigue damage. The elastic modulus and static strength remain intact up to, and probably beyond, two million cycles. Above the shakedown stress level there is a damage accumulation region, where reductions in the elastic modulus are observed after a certain number of cycles. The S-N curve is a boundary between the damage accumulation region and the fracture region. Graphs, similar to Fig. 13, can be constructed for other laminates and material systems and would be useful for designing MMC components.

If a designer only concerned himself with the materials S-N fatigue behavior shown in Fig. 13, he would chose 70% of ultimate as a safe design load for a life up to at least 2 million cycles. However, the MMC would experience a significant loss of stiffness. If the designer wished to retain all of the initial stiffness for the 2 million cycle lifetime, then he should not allow the cyclic stress range to exceed 35% of ultimate for this particular composite.

The presented results also indicate that matrix damage at notch tips can be predicted using the shakedown criteria. Matrix damage can occur on a local scale at the notch tip.

Fiber Dominated Damage

FP/aluminum data

In alumina fiber/aluminum composites, the alumina fibers (denoted as FP by DuPont) are very small in diameter (0.02 mm) compared to the boron fibers (0.140 mm) and have a lower static strain to failure (approximately 0.003). The surface of an alumina fiber is "cobblestone" like, which may imply a low fatigue strength due to stress concentrations. In this composite system, the fibers may very well fail due to fatigue before the matrix does, thus, fatigue damage would be fiber dominated.

Tsangarakis, Slepetz, and Nunes [19] investigated the fatigue behavior of two different batches of an alumina fiber reinforced aluminum composite (FP/Al). This section will essentially be a review of their work. Both batches that they tested had a nominal fiber volume fraction of 55% with the fibers uniaxially oriented in the loading direction. The matrix is an Al-2.5%Li alloy. Tension-tension fatigue tests were conducted on flat, untabbed, contoured specimens at R=0.1. Some specimens were strain gaged so that the load-strain response could be monitored during the fatigue tests. Metallographic and fractographic examinations of the specimens were conducted to evaluate failure modes and damage mechanisms.

Fig. 14 presents fatigue data that show a significant difference in mechanical properties of the two batches of FP/Al investigated. The first batch had an endurance limit (as indicated by the runout data points) of 410 MPa compared to 330 MPa for the second batch. The static strength and modulus were correspondingly higher for the first batch than the second. Fatigue cycling did not cause a decrease of secant modulus in either batch of material, contrary to the reported behavior for B/Al [3]. Fiber failure was found to dominate the fatigue life of FP/Al, and failure of the composite generally occurred after a sufficient number of fibers fractured at a given cross section.

The most significant damage in both failed and runout specimens of FP/Al was extensive fiber fracture, including multiple fractures of individual fibers. Even though many of the fibers were broken, some in several places, they were able to pick-up and carry load very effectively. This is evident from the fact that the secant modulus remained essentially unchanged until just prior to laminate failure despite considerable fiber fracture. This implies that the matrix and fiber remained well bonded.

The difference in the fatigue behavior of FP/Al and B/Al is due to the differences in fiber properties. The tensile modulus of the FP fiber is 379 GPa (close to the 400 GPa modulus of the boron fibers) but the strength is approximately 1.38 GPA (boron's strength is approximately 3.45 GPa.) The failure strain for boron fibers is over twice that of the alumina fibers. Their respective fatigue strengths have perhaps the same ratio. On the other hand, the shakedown stress range is nearly equal for the two systems because both have essentially the same matrix yield strength and composite modulus. Therefore, fatigue failures can occur in the fibers of the FP/Al composite at stress levels below the shakedown range defining the threshold level for matrix fatigue. The larger and stronger boron fibers have greater resistance to crack propagation and deflect the crack along the fiber/matrix interface in B/Al. This results in a very erratic crack path (not flat), featuring some debonding and fiber pullout prior to fatigue failure. In the FP/Al composite, the combination of weaker, smaller diameter fibers and a stronger interface make it easier for a fatigue crack to propagate across fibers on relatively flat planes as shown in Fig. 15.

In summary, progressive fiber fracture was found to be the dominant damage mechanism controlling the fatigue behavior of FP/Al. Once a sufficient number of broken fibers developed at a cross section, composite failure occurred.

Silicon-carbide/titanium data

Recent work on a silicon-carbide fiber reinforced titanium matrix composite (SCS_6/Ti-15-3) [20] has shown that the stress level in the 0^o plies may be a governing parameter for predicting fatigue life. S-N data was experimentally determined for four different lay-ups containing 0^o plies as shown in Fig. 16. The stress-strain response was monitored during the fatigue life. The stiffness dropped very early in the cycling history due to fiber/matrix interface separations. (This will be discussed in greater detail in the next section.) Fatigue cracks in the matrix, such as those observed in B/Al, were not observed in this materials system. After a few cycles the stiffness stabilized and the cyclic strain range was recorded. This stabilized strain range was multiplied by the fiber modulus (400 GPa) to determine the cyclic stress range in the fiber. The number of cycles to failure was then plotted against the cyclic stress in the 0^o fibers. The fatigue data from the four

different laminates was correlated very well by the 0^{o} fiber stress as shown in Fig. 17. This correlation makes a lot of sense since the laminate will not fail until the 0^{o} fiber fails. Therefore, it is reasonable to assume that the stress in the 0^{o} fiber will dictate fatigue life.

It is important to note that the fiber failures were not the first damage to occur in these composites. The first damage that caused significant modulus changes was the failure of the fiber/matrix interface in the off axis plies.

Self-Similar Fatigue Damage Growth

Titanium matrix MMC are very attractive because of their high stiffness and high temperature capabilities. Ti-6Al-4V has an elastic modulus of 110 GPa. Thin sheet (1.60 and 3.18 mm) Ti-6Al-4V has a tensile yield strength of 1089 MPa [21]. This implies a strain to yield of approximately 0.01. This strain is well above the strain to failure of boron or silicon-carbide fibers. However, the fatigue endurance limit at 10^{7} cycles for titanium is approximately 600 MPa [21]. In this case, the strain to the matrix fatigue limit is close to the fiber failure strain. Since the fatigue limit is significantly lower than the yield stress, the matrix may develop fatigue cracks without yielding the matrix globally. Furthermore, the titanium is much stronger than the typical aluminum matrix material, and is therefore capable of creating a much higher stress concentration in a fiber ahead of a matrix crack.

Considering the closeness of the strains for failure of the matrix and fiber and the high stress concentration capabilities of the titanium (because of the high strength of titanium, a matrix crack is more capable of creating a high stress concentration in an adjoining fiber than would be a weaker matrix system such as aluminum), it is not surprising that Saff and Grimsley [22] reported self-similar crack growth for notched unidirectional boron/titanium composites (B_4C/6-4 titanium) subjected to fatigue loadings. (They also reported that in some cases fibers failed before the matrix under fatigue loading.) Saff [17] reported that the crack growth in titanium MMC was often self-similar as in metals. A comparison of crack growth rate data from center cracked panels of the MMC and the parent matrix material (Fig. 18) indicates that the MMC requires higher loads to reach threshold, and provides much slower crack growth rates for most of the life. However the figure also shows that the MMC has a lower fracture toughness. Saff felt that the higher thresholds are controlled by the fiber/matrix interface strength (the lower the interface strength, the higher the threshold) because the matrix can not transfer crack tip strains to the fiber when the interface is weak.

Saff also suggests that the overall crack growth is controlled by the fiber/matrix interface and the fiber spacing. He found examples of bundles of fibers inhibiting crack growth in the titanium MMC. The bundles essentially halted the crack growth across the fibers and forced the crack to grow parallel to the fibers until weaker fiber sections allowed the crack growth to continue across the fibers again. This process may cause an apparent acceleration in crack growth when the fiber bundle fails and releases energy into the matrix once again. The ability of the crack to change paths depends on the crack length and the fiber/matrix interface strength.

Another explanation for the slower crack growth rate of the titanium MMC shown in Fig. 18 is fiber pull-out. The crack growth failure surface is seldom perfectly flat, and most surfaces have at least a small amount of fiber pull-out. In addition there may well be some fractured fiber fragments embedded in the surface. This may prevent the crack from closing as fully as the parent material alone would. This results in a debris (or surface roughness) induced closure phenomenon [23] that essentially causes the crack growth rate to slow down.

The author also found evidence of self-similar crack growth in as-fabricated unnotched unidirectional specimens of SCS_6/Ti-15-3 material. The fatigue data, which was shown in Fig. 17, indicates that a SCS_6 fiber may have a fatigue endurance limit around 1300 MPa. Since the fiber modulus is approximately 400 GPa, the endurance strain range for the fiber is 0.0033. Fatigue tests conducted by the author on the Ti-15-3 material without fiber reinforcement indicates a fatigue endurance strain range of approximately 0.0036 at R=0.1. Thus, the approximated endurance strain ranges for the fiber and matrix are very nearly the same. Figure 19 presents a photograph of a portion of a unidirectional specimen failure surface. Half of the failure surface was rather bright, indicating the surface had failed in fatigue. The other half was rather dull as is typical of a dimpled surface indicating static failure. The portion of the failure surface shown in Fig. 19 laid within the brighter fatigue area. Specifically the photo shows where a semi-circular shaped crack intersected a larger crack that was growing from one edge of the specimen (growing from right to left in the photograph.) This is a good illustration of damage initiating and growing as a self-similar crack. The next section will discuss how these composites have rather weak fiber/matrix interfaces. However, due to a combination of the residual radial compressive matrix stresses around the fiber (discussed in more detail in the next section) and the Poisson effect of pulling a unidirectional laminate in tension, the interface was sufficiently strong to allow self-similar crack growth in these unidirectional laminates.

Fiber/Matrix Interface Failures

This section will review some of the work reported by the author and his colleagues [24] on the mechanical behavior of a titanium MMC (SCS_6/Ti-15-3). The initial stress-strain curves for each laminate containing off-axis plies exhibited a knee in the loading curve at approximately 140 MPa, well below the matrix material's minimum yield strength of 690 MPa. In all cases, the unloading elastic modulus was also less than the initial elastic modulus, thus indicating that some sort of damage had occurred in the laminate. Figure 20 shows the initial loading-unloading curve for a $[90]_8$ laminate. There is a small amount of residual permanent strain, thus the unloading curve does not coincide with the loading curve. After the first cycle, the unloading curve closely followed the loading curve (as shown for the 11^{th} cycle in Fig. 21) indicating an opening and closing phenomenon. This loading and unloading results in a nearly bilinear response with a knee in the area of 110 MPa. It was thought that the fiber/matrix interface may be failing in the off-axis plies. This was confirmed using the edge replica technique.

Edge replicas were taken at various stages of the quasi-static load history of a specimen and were examined using scanning electron microscope. Figure 22 shows edge replicas of the $[90]_8$ laminate taken at no load and at 276 MPa. In the micrograph taken at 276 MPa, there is a noticeable amount of acetate protruding from gaps between the fiber and the matrix. However, at no load, there are no discernible gaps. Although this technique only shows what is the state at the surface of the specimen, the stiffness change shown in Fig. 21 is large enough to indicate that the fiber/matrix separation occurs throughout the specimen.

Figure 23 shows the fiber/matrix separation for a typical 90^o fiber in a $[0/90]_{2s}$ laminate under load. Figure 24 presents the fiber/matrix separation for a sequence of loads in the $[0/\pm45/90]_s$ laminate. The unloaded specimen shows no evidence of fiber/matrix separation. (Notice in this figure that there are a number of chipped places in the fiber that also show-up in the photos of the loaded specimen.) At 207 MPa there is significant fiber/matrix separation in the 90^o plies, but practically none in the 45^o plies. At 414 MPa, there is much more separation in the 90^o plies and some noticeable separation in the 45^o plies. In general, the 90^o plies experience fiber/matrix separation at a lower level of laminate stress than do the 45^o plies. The 90^o fibers develop much higher transverse stresses (stresses that act to separate the fiber from the matrix) than do the 45^o fibers in the same loaded laminate. This type of behavior was typical of laminates containing off-axis plies.

This still does not explain why the fiber/matrix separation closes while unloading. Residual thermal stresses were suspected; therefore, the cylindrical fiber model described in Ref 24 was used

to estimate these stresses. For the analysis of the silicon carbide/ titanium material system, a coefficient of thermal expansion of 4.86 x 10^{-6} cm/cm/^{o}C was used for the fiber and 9.72 x 10^{-6} cm/cm/^{o}C [25] was used for the matrix. It was assumed that any stresses that might develop during the fabrication process at absolute temperatures greater than one half of the melting point of the matrix would be relieved due to creep [26]. Therefore, a temperature change of 555^{o}C was used. For the as-fabricated unidirectional laminate the analysis predicted the following stresses in the matrix material near the fiber/matrix interface: the radial stress was -138 MPa, the tangential stress was 276 MPa, and the axial stress in the fiber direction was 207 MPa. The compressive radial stress and tensile tangential (hoop) stress would cause the fiber and matrix to rejoin upon unloading after the interface failed. Even if the fiber/ matrix interface has failed, these residual stresses must be overcome before the fiber and matrix can separate.

From this analysis, we see that the matrix is "choking" the fiber. A stress of approximately 138 MPa in the 90^{o} lamina is required to overcome the residual radial stresses around the fiber to allow the fiber/matrix separation to occur. The cylindrical fiber model estimated the residual axial stress in the matrix to be 207 MPa and the tangential stress to be 276 MPa. These residual stresses are not large compared to a yield strength of at least 690 MPA. Therefore, the knee in the laminate stress-strain curve at approximately 138 MPa is caused almost entirely by fiber/matrix separation and not by matrix plasticity.

Matrix cracking causes similar stiffness losses and loading-unloading responses for boron/aluminum [4] and silicon-carbide/aluminum [5] composites. However, for these systems, it took thousands of cycles to develop damage equivalent to that occurring in just a few cycles for the SCS_6/Ti-15-3 system. Figure 25 presents a plot of the elastic unloading modulus (E_{ul}) divided by the initial elastic modulus (E_I) versus the number of applied cycles. As previously discussed, the elastic unloading modulus is a good indicator of the amount of damage in a composite. The elastic unloading modulus would be equal to the initial elastic modulus if the composite was undamaged. The data is from $[0/90]_{2s}$ laminates of boron/aluminum (B/Al) [1] and the SCS_6/Ti-15-3 [24]. Both laminates are loaded such that the ratio of stress range to ultimate strength is approximately the same. In the case of the B/Al laminate, damage initiated in the matrix material of the off axis plies and grew as a fatigue crack. Therefore, the B/Al stiffness did not drop during the number of cycles required for fatigue crack initiation. Thereafter, the modulus slowly dropped with an increasing number of cycles until at 2 million cycles the unloading modulus had dropped by almost 20 percent. This is in sharp contrast to the Ti-15-3 composite for which the modulus dropped 20 percent in the first few cycles, then remained almost

constant until just before failure at 10,000 cycles. This is a good example of how failure mode affects laminate stiffness.

Since the aluminum matrix composites did not have these extensive fiber/matrix interface failures, the interfaces in the boron/aluminum or silicon-carbide/aluminum composites [4,5] may be much stronger than the interface between the SCS_6 fibers and the Ti-15-3 matrix material. The actual strengths of these interfaces are not well defined at this time and, therefore, can not be compared. However, it can be shown that the titanium matrix composite demands much more strength from the fiber/matrix interface than does an aluminum matrix composite. From the AGLPLY analysis, the matrix stress, in the loading direction, in the 90^{o} ply of a $[0/90]_{2s}$ laminate is shown in Fig. 26. This stress is approximately equal to the stress at the fiber/matrix interface. The aluminum matrix can not support a load much above its matrix yield strength of approximately 138 MPa. Therefore, the 90^{o} fibers do not have to carry any more load than the matrix can support. However, the titanium has a very high yield strength, thus much higher loads are carried in the 90^{o} plies and transferred into the fibers. For a given laminate stress level, it is clear that in titanium matrix composites, the fiber/matrix interface is more highly stressed than in aluminum matrix composites. In order for the full potential of titanium matrix composites to be realized, the fiber/matrix interface must be made significantly stronger than the system reported on herein.

SUMMARY

This paper reviewed some techniques for conducting meaningful fatigue tests to detect and quantify fatigue damage in MMC. These techniques included interpretation of stress-strain responses, acid etching of the matrix, edge replicas of the specimen under load, radiography, and micrographs of the failure surfaces. The paper also showed how stiffness loss in continuous fiber reinforced metal matrix composites is a useful parameter for detecting fatigue and quantifying damage initiation and accumulation. Numerous examples of how fatigue damage can initiate and grow in various MMC were given. Depending on the relative fatigue behavior of the fiber and matrix, and the interface properties, the failure modes of MMC can be grouped into four categories: (1.) matrix dominated, (2.) fiber dominated, (3.) self-similar damage growth, and (4.) fiber/matrix interfacial failures. These four types of damage were discussed and illustrated by examples. Some key observations about fatigue damage in continuous fiber reinforced MMC are listed below.

- Matrix dominated damage occurs if the matrix material has a lower fatigue endurance strain range than does the fiber. This results in the development of matrix cracks that can cause significant losses in stiffness in laminates with off-axis plies without actually failing 0^{o} fibers or resulting in

laminate failure.

- Fiber dominated damage occurs if the fiber has a lower fatigue endurance strain range than does the matrix material. In this case numerous fiber breaks may occur within the laminate, yet the stiffness may be relatively unaffected if the broken fibers are able to effectively pick-up load. This type of damage results in sudden laminate failure.

- Self-similar crack growth can occurs if the fiber and matrix materials have similar values fatigue endurance strain ranges. The material can experience crack growth much like a crack in a homogeneous material.

- Fiber/matrix interfaces will fail if they are weaker than the transverse strength of the fiber and the matrix. The higher the strength of the matrix material the greater the chance of interfacial failures in the off-axis plies. This type of damage can result in a significant loss of stiffness during the first cycle for a laminate containing off-axis plies.

ACKNOWLEDGMENT

The author would like to acknowledge Steve Lubowinski and Mary Swain of Planning Research Corporation, Hampton, Virginia, for helping conduct the fatigue tests and photographing the failure surface, respectively, of the SCS_6/Ti-15-3 composite specimens.

REFERENCES

[1] Johnson, W. S., Characterization of Fatigue Damage Mechanisms in Continuous Fiber Reinforced Metal Matrix Composites, Ph.D. Dissertation, Duke University (1979).

[2] Dvorak, G. J. and Johnson, W. S.,"Fatigue of Metal Matrix Composites," International Journal of Fracture, Vol. 16, No. 6, Dec. 1980, pp. 585-607.

[3] Johnson, W. S., "Mechanisms of Fatigue Damage in Boron/Aluminum Composites," Damage in Composite Materials, ASTM STP 775, K. L. Reifsnider, Ed., American Society for Testing and Materials, Philadelphia, 1982, pp. 83-102.

[4] Johnson, W. S., "Modeling Stiffness Loss in Boron/Aluminum Laminates Below the Fatigue Limit", Long-Term Behavior of Composites, ASTM STP 813, T. K. O'Brien, Ed., American Society of Testing and Materials, Philadelphia, 1983, pp. 160-176.

[5] Johnson, W. S. and Wallis, R. R., "Fatigue Behavior of Continuous Fiber Silicon Carbide/Aluminum Composites," Composite Materials: Fatigue and Fracture, ASTM STP 907, H. T. Hahn, Ed., American Society for Testing and Materials, Philadelphia, 1986, pp.161-175.

[6] O'Brien, T. K., "Effect of Gage-Section Size on Composite Stiffness Measurements," Composites Technology Review, Vol. 1, No. 4, 1979, pp.5-6.

[7] Johnson, W. S., Bigelow, C. A., and Bahei-El-Din, Y. A., Experimental and Analytical Investigation of the Fracture Processes of Boron/Aluminum Laminates Containing Notches, NASA TP 2187, National Aeronautics and Space Administration, Washington D.C., 1983.

[8] Awerbuch, J., "On the Applicability of Acoustic Emission for Monitoring Damage Progression in Metal Matrix Composites," Metal Matrix Composites: Testing, Analysis and Failure Modes, ASTM STP 1032, W. S. Johnson, Ed., American Society for Testing and Materials, Philadelphia, 1989.

[9] Dvorak, G. J. and Tarn, J. Q., "Fatigue and Shakedown in Metal Matrix Composites," Fatigue of Composite Materials, ASTM STP-569, American Society for Testing and Materials, Philadelphia, 1975, pp.145-168.

[10] Dvorak, G. J. and Johnson, W. S.,"Fatigue Mechanisms in Metal Matrix Composite Laminates," Advances in Aerospace Structures and Materials, ASME AD-01, American Society of Mechanical Engineers, New York, 1981, pp. 21-34.

[11] Aluminum, Vol 1, K. R. Van Horn, ed., American Society for Metals, Metals Park, Ohio (1967) 183.

[12] Weng, M. T., "Some Aspects of Fatigue Relative to Cyclic Yield Stress," International Journal of Fatigue," Vol. 3, No. 3, Oct. 1981, pp. 187-193.

[13] Bahei-El-Din, Y. A. and Dvorak, G. J., "Plasticity Analysis of Laminated Composite Plates," ASME Journal of Applied Mechanics, Vol.49, 1982, pp. 740-746.

[14] Bahei-El-Din, Y. A., Plastic Analysis of Metal Matrix Composite Laminates,Ph.D. Dissertation, Duke University (1979).
[15] Wung, C. J., "Strain-Space Analysis of Plasticity, Fracture, and Fatigue of Fibrous Composites," Ph.D. Dissertation, University of Utah, March 1987.
[16] Grimsley, F. M., Static and Fatigue Behavior of Pin-Loaded Metal Matrix Joints, AFWAL-TR-84-3063, Air Force Wright Aeronautical Laboratories, 1984.
[17] Harmon, D. M., Saff, C. R., and Sun, C. T., Durability of Continuous Fiber Reinforced Metal Matrix Composites, AFWAL-TR-87-3060, Air Force Wright Aeronautical Laboratories, 1987.
[18] Simonds, R. A., Residual Strength of Five Boron/Aluminum Laminates with Crack-Like Notches After Fatigue Loading, NASA CR 3815, National Aeronautics and Space Administration, Washington D.C., July 1984.
[19] Tsangarakis, N., Slepetz, J. M., and Nunes, J., "Fatigue Behavior of Alumina Fiber Reinforced Aluminum Composites," Recent Advances in Composites in the United States and Japan, ASTM STP-864, J. R. Vinson and M. Taya, Eds., American Society for Testing and Materials, Philadelphia, 1985, pp. 131-152.
[20] Johnson, W. S., Lubowinski, S. J., and Brewer, W. D., "Mechanical Characterization of Ti-15-3/SCS_6,"Fourth National Aero-Space Plane Symposium, Volume IV - Materials, NASP CP 4025, February 1988, pp. 357-380.
[21] Ruff, P. E., Metrification of MIL-HDBK-5C, AFWAL-TR-80-4110, Air Force Wright Aeronautical Laboratories, 1980.
[22] Saff, C. R., and Grimsley, F. M., Testing Technology of Metal Matrix Composites, ASTM STP-964, American Society for Testing and Materials, Philadelphia, 1988.
[23] Walker, N. and Beevers, C. J., Fatigue of Engineering Materials and Structures, Vol. 1, 1979, pp.135-148.
[24] Johnson, W. S., Lubowinski, S. J., Highsmith, A. L., Brewer, W. D., and Hoogstraten, C. A., Mechanical Characterization of SCS_6/Ti-15-3 Metal Matrix Composites at Room Temperature, NASP TM 1014, 1988.
[25] Rosenberg, H. W., "Ti-15-3: A New Cold-Formable Sheet Titanium Alloy," Journal Of Metals, Vol. 35, No. 11, November 1986, pp.30-34.
[26] Dieter, G.E., Mechanical Metallurgy, 2nd ed., McGraw-Hill, New York, 1976, pp.451-489.

APPENDIX

Matrix damage model: The model starts by assuming that the matrix is cycling plastically. As cracks develop due to plastic cycling, the effective modulus is reduced for the portion of the matrix cycle that is in tension. The model presents simple equations to approximate the effective matrix modulus due to cracking at an assumed cyclic strain range. The program AGLPLY [13] is used to calculate the laminate response with the effective modulus of the fatigued matrix. Thus a bilinear response, such as shown in Fig. 2 for 500,000 cycles, can be computed. The secant modulus is calculated from the bilinear response.

Figure 27 illustrates this behavior in terms of the applied laminate stress and the corresponding axial stresses in the matrix and 0^o fibers. The dashed lines in Fig. 27 represent the initial loading response. Accordingly, the first load cycle causes the matrix and 0^o fiber stresses to follow the dashed loops. The laminate has an ideally elastic-plastic matrix (for illustration of the model and simplicity of presentation) and is subjected to a constant cyclic stress range, ΔS. The dashed loops are for the same condition represented in Fig. 2 for the fourth cycle. σ_{Sh}^m is assumed to be the axial stress in the matrix material in the loading direction at the shakedown stress limit ΔS. (The matrix is yielded at this point by a combination of axial and shear stresses.) Assuming the matrix yields at the same value in tension and compression, σ_{Sh}^m equals half of the laminate's shakedown strain range $\Delta S_{Sh}/E_0$ times the matrix tensile modulus, E^m.

$$\sigma_{Sh}^m = \Delta S_{Sh}/2E_0 \times E^m \qquad (1)$$

The ΔS_{Sh} in this equation is the shakedown stress range, E_0 is the undamaged laminate's elastic modulus in the loading direction, and E^m is the undamaged matrix's elastic modulus. With subsequent cycling, the cyclic plasticity causes matrix cracks to initiate and grow, effectively decreasing the matrix tensile modulus until a saturation damage state is reached. The dashed loops in Fig. 27 narrow to zero-width loops shown as solid lines, which represent the saturation damage state. These solid lines correspond to the laminate cyclic stress-strain response illustrated in Fig. 2 for the 500 000th cycle. The saturation damage state develops when the matrix cracking causes the load to transfer to the 0^o fibers, thus relieving the matrix from undergoing additional damaging plastic deformation.

The drop in matrix modulus in the load direction due to fatigue damage can now be determined using Fig. 28. The strain in the matrix and laminate is plotted versus the matrix stress σ^m or the laminate stress S. The damage state has an associated cyclic strain range, $\Delta\epsilon$. If this cyclic strain range is assumed, an effective tensile modulus of the matrix material E^m_{eff} can be estimated. This

assumes that the same SDS will be reached by either stress or strain control. Note that E^m_{eff} is the modulus in the loading (0^o fiber) direction. The compressive strain range of the matrix $\Delta\epsilon^m_{comp}$ was approximated as

$$\Delta\epsilon^m_{comp} = \Delta S_{Sh}/2E_0. \tag{2}$$

The effective tensile modulus of the matrix material can now be approximated by dividing σ_{Sh}^m by the cyclic strain minus the compressive portion.

$$E^m_{eff} = \sigma_{Sh}^m/(\Delta\epsilon - \Delta\epsilon^m_{comp}) \tag{3}$$

E^m_{eff} is used as the matrix modulus in lamination theory (using the computer program AGLPLY) to calculate E_{SDS}, the unloading elastic modulus of the composite in its saturation damage state (at approximately 500 000 cycles). The shear modulus of the matrix is also reduced within AGLPLY based on E^m_{eff} and Poisson's ratio. All the fibers were assumed to be intact, and the matrix damage was assumed to be characterized by the laminate's lowered modulus, E^m_{eff}. Although such a formulation implicitly assumes that the matrix modulus is reduced isotropically, the reduction actually is orthotropic. However, the interest is in the laminate modulus in the primary loading direction only, and the assumption should not introduce excessive error.

Returning to Fig. 28, we now know the modulus for each of the two linear segments, as well as the strain ranges. Therefore, the overall laminate stress range ΔS can be calculated as follows

$$\Delta S = (\Delta\epsilon^m_{comp})E_0 + (\Delta\epsilon - \Delta\epsilon^m_{comp})E_{SDS} \tag{4}$$

Equation (4) is rewritten using Eq (2).

$$\begin{aligned} \Delta S &= E_{SDS}\Delta\epsilon + 1/2\ \Delta S_{Sh}(1 - E_{SDS}/E_0) && \text{for } \Delta S > \Delta S_{Sh}/2 \\ &= E_0\Delta\epsilon && \text{for } \Delta S \leq \Delta S_{Sh}/2 \end{aligned} \tag{5}$$

The values of ΔS_{Sh}, E_0, and E_{SDS} were calculated using AGLPLY. Equation (5) applies to either stress- or strain-control cycling. By selecting a number of different strain range values $\Delta\epsilon$, the corresponding laminate stress range ΔS can be calculated and plotted versus $\Delta\epsilon$. The laminate secant modulus then is

$$E_S = \Delta S/\Delta\epsilon. \tag{6}$$

Numerous examples of correlation of this model with experimental data are given in Refs 4 and 5.

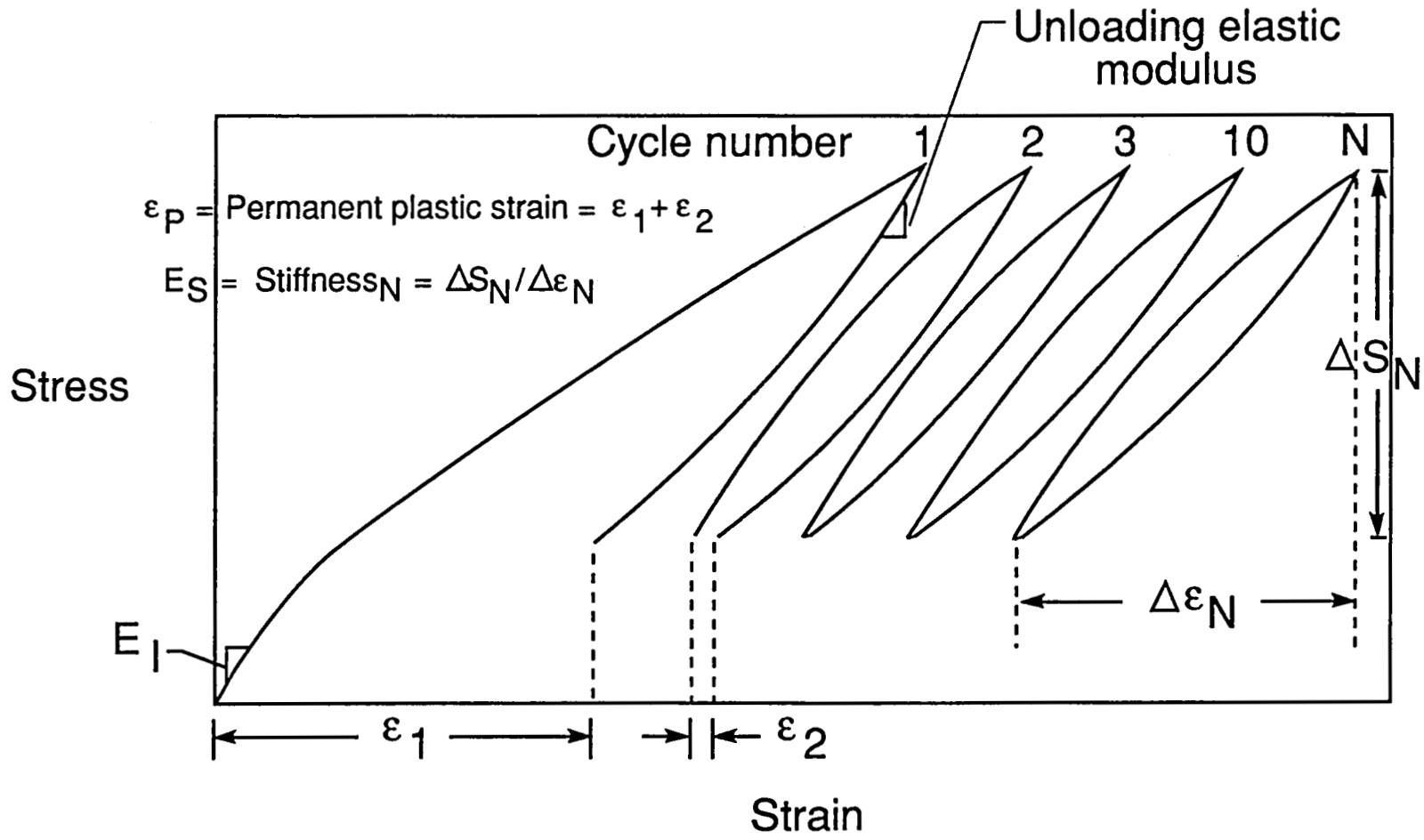

Figure 1 - Example stress-strain recording of a B/Al laminated composite specimen [1].

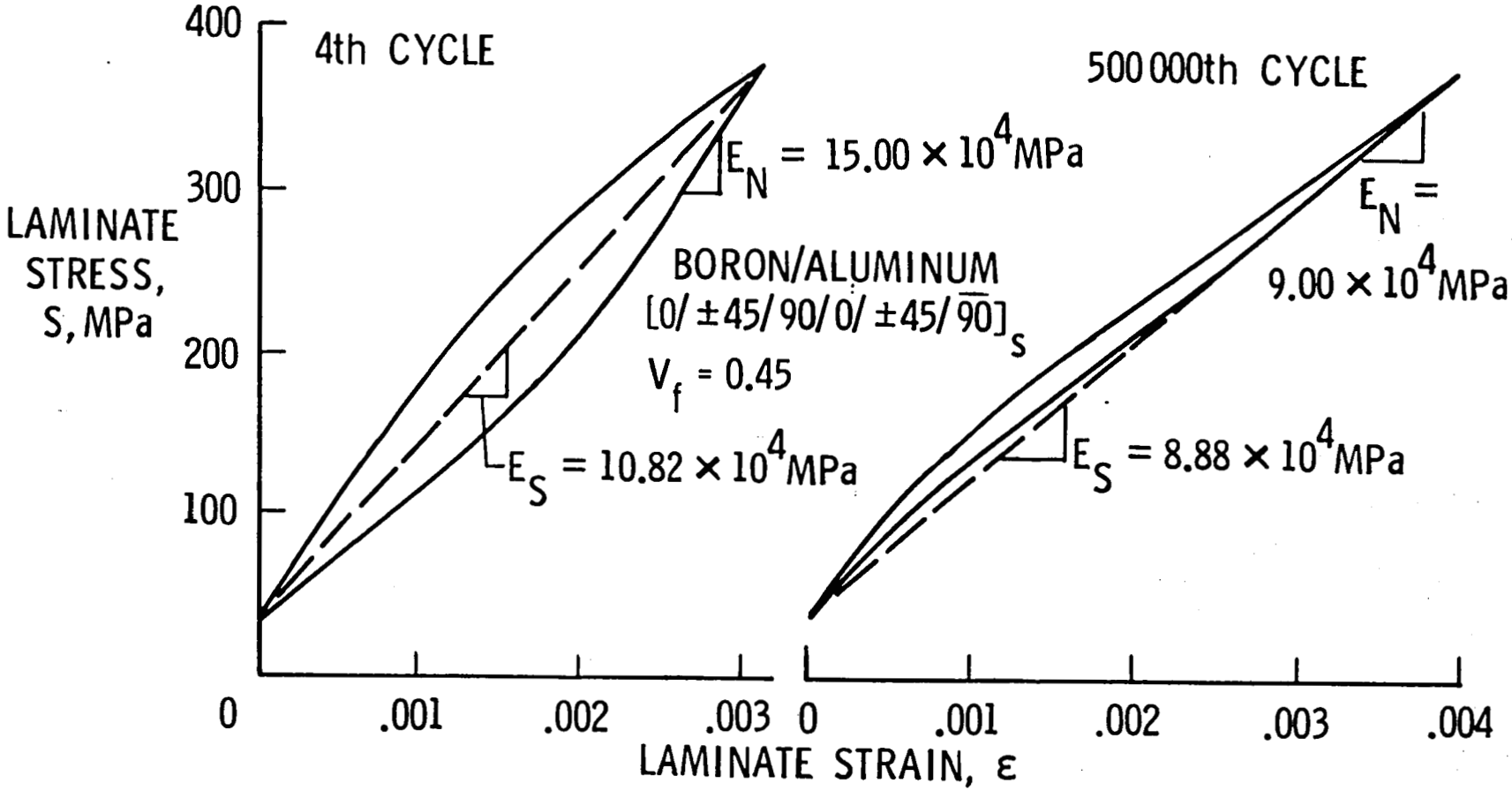

Figure 2 - Observed S-ε response in the fourth cycle due to plasticity and in the 500,000th cycle due to matrix cracking [4].

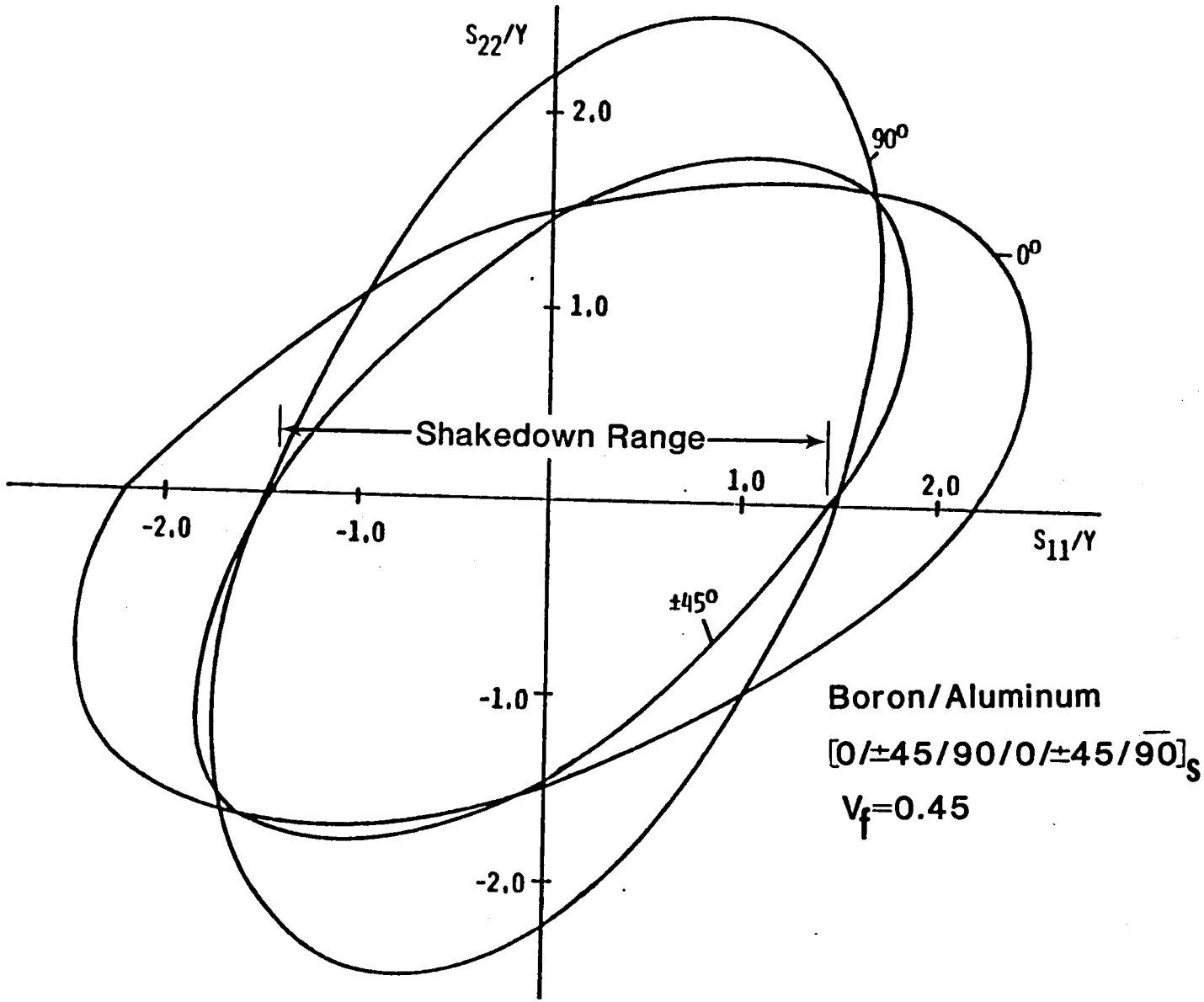

Figure 3 - Yield surfaces of a B/Al laminate loaded by in-plane biaxial normal stresses. The S_{11} direction coincides with the 0° fiber direction [2].

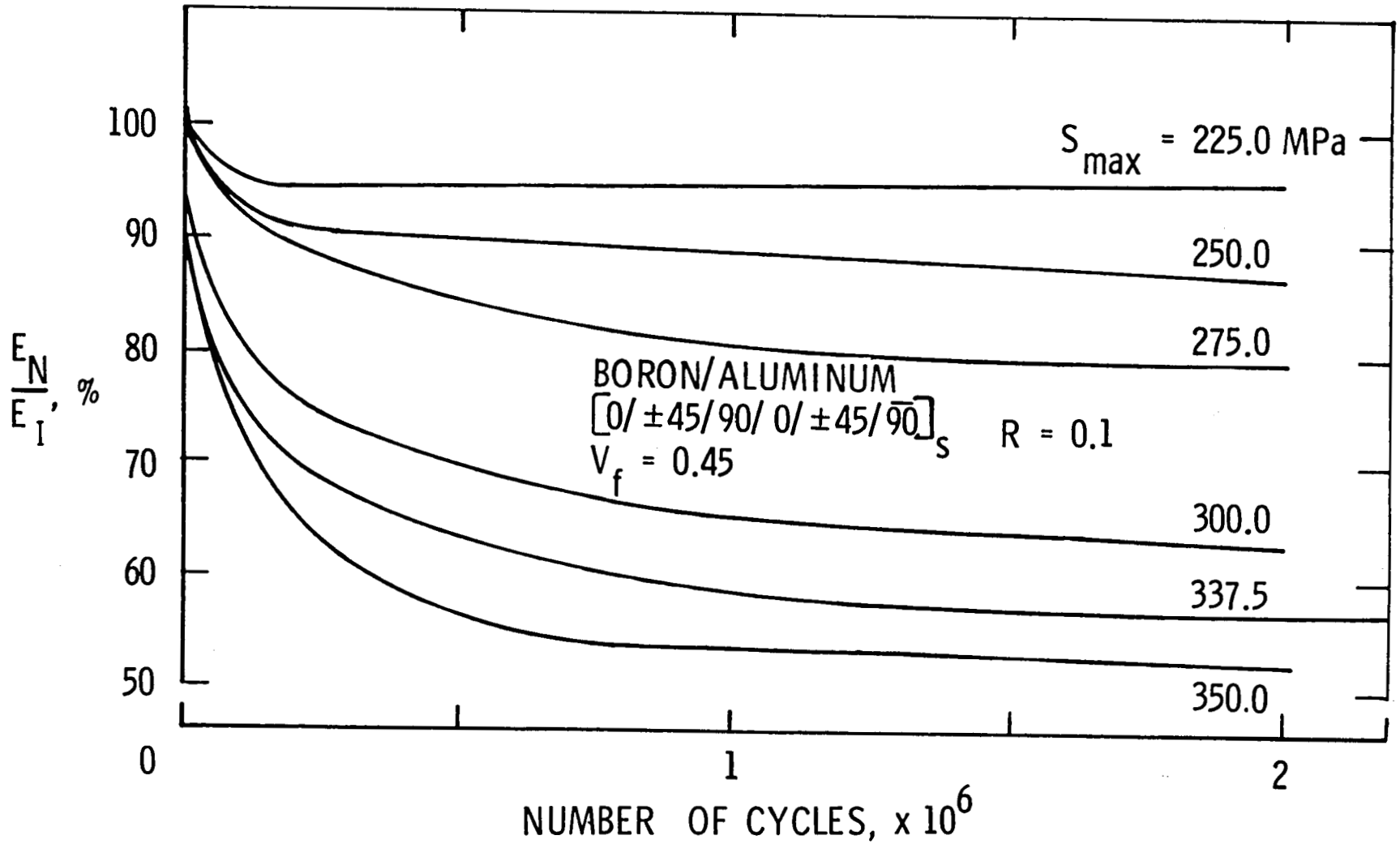

Figure 4 - Percentage of the initial elastic unloading modulus retained as a function of applied cycles [1].

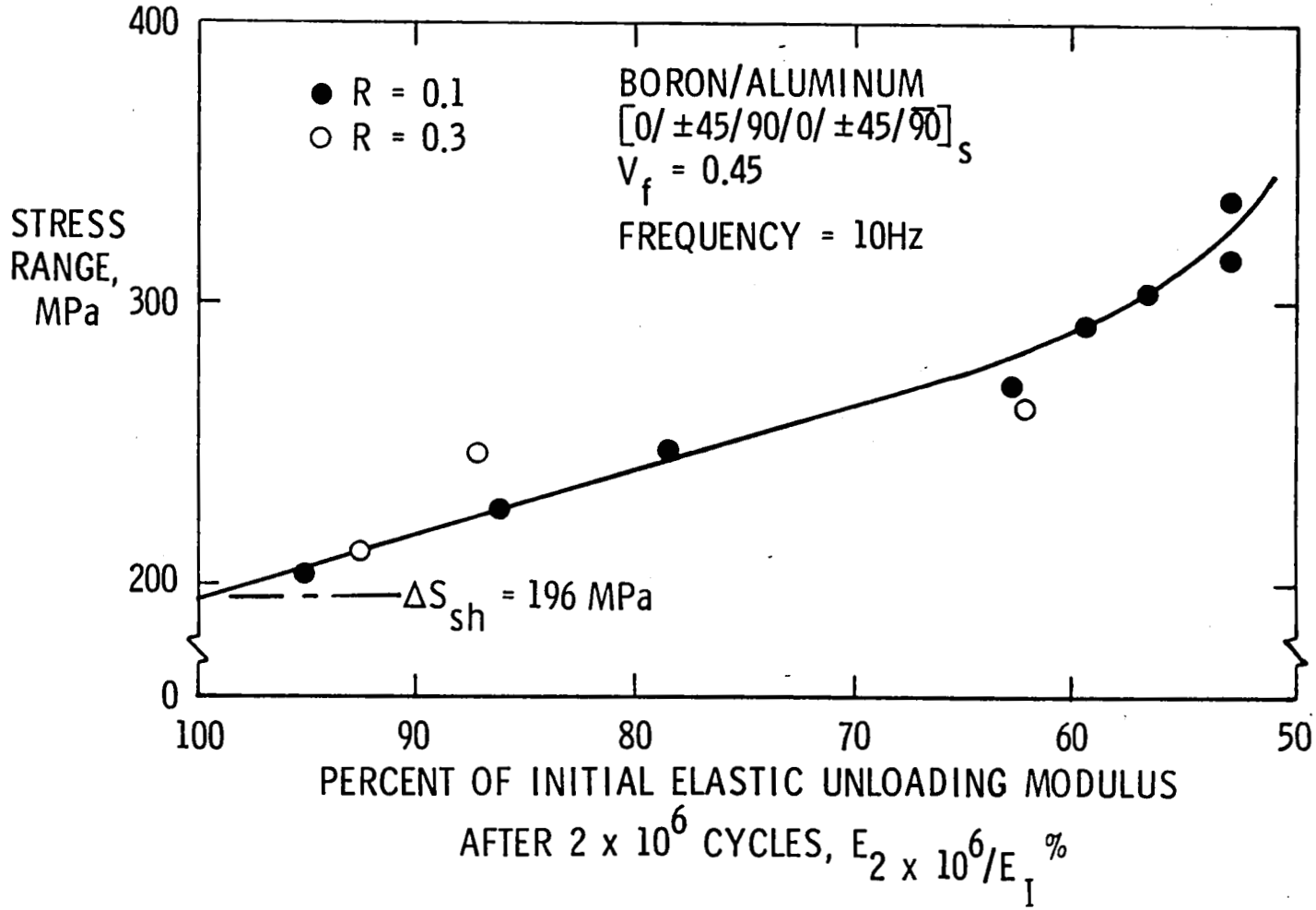

Figure 5 - Percentage of the initial elastic unloading modulus retained after 2 million cycles as a function of applied stress range [1].

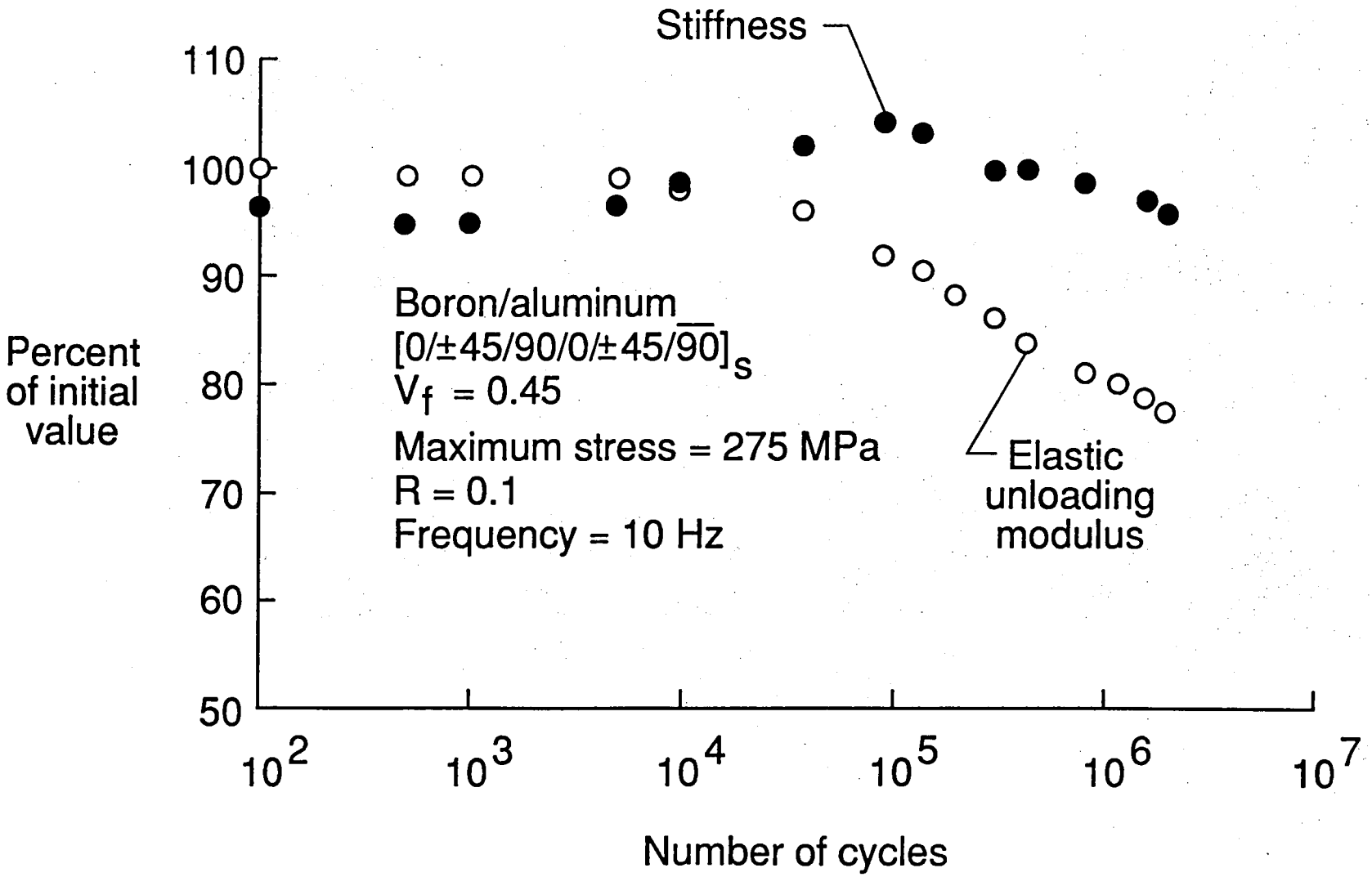

Figure 6 - Comparison of the changes in elastic unloading modulus and stiffness as a function of applied cycles [1].

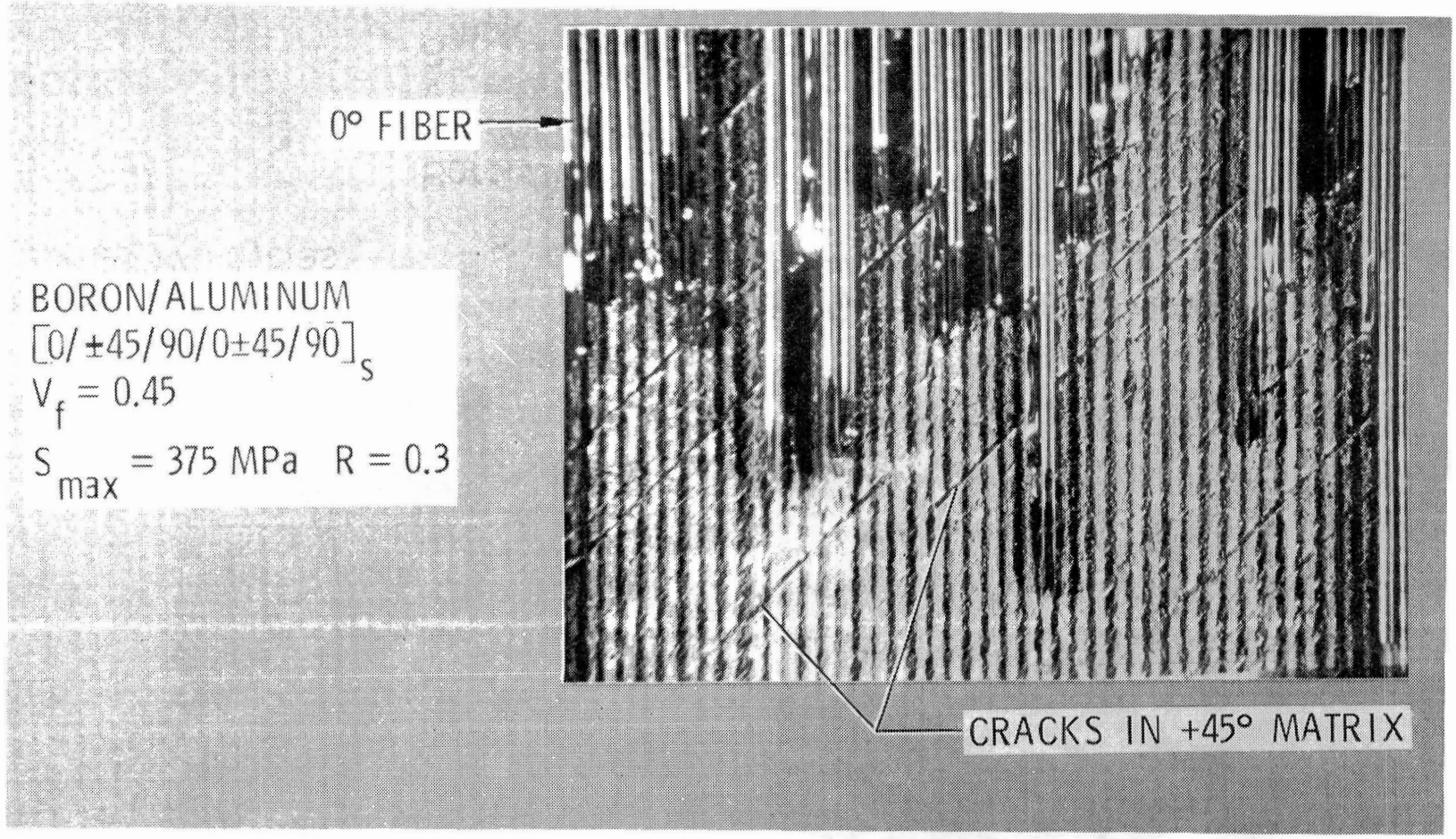

Figure 7 - Matrix cracks in the +45° lamina as exposed by etching away the 0° matrix material [3].

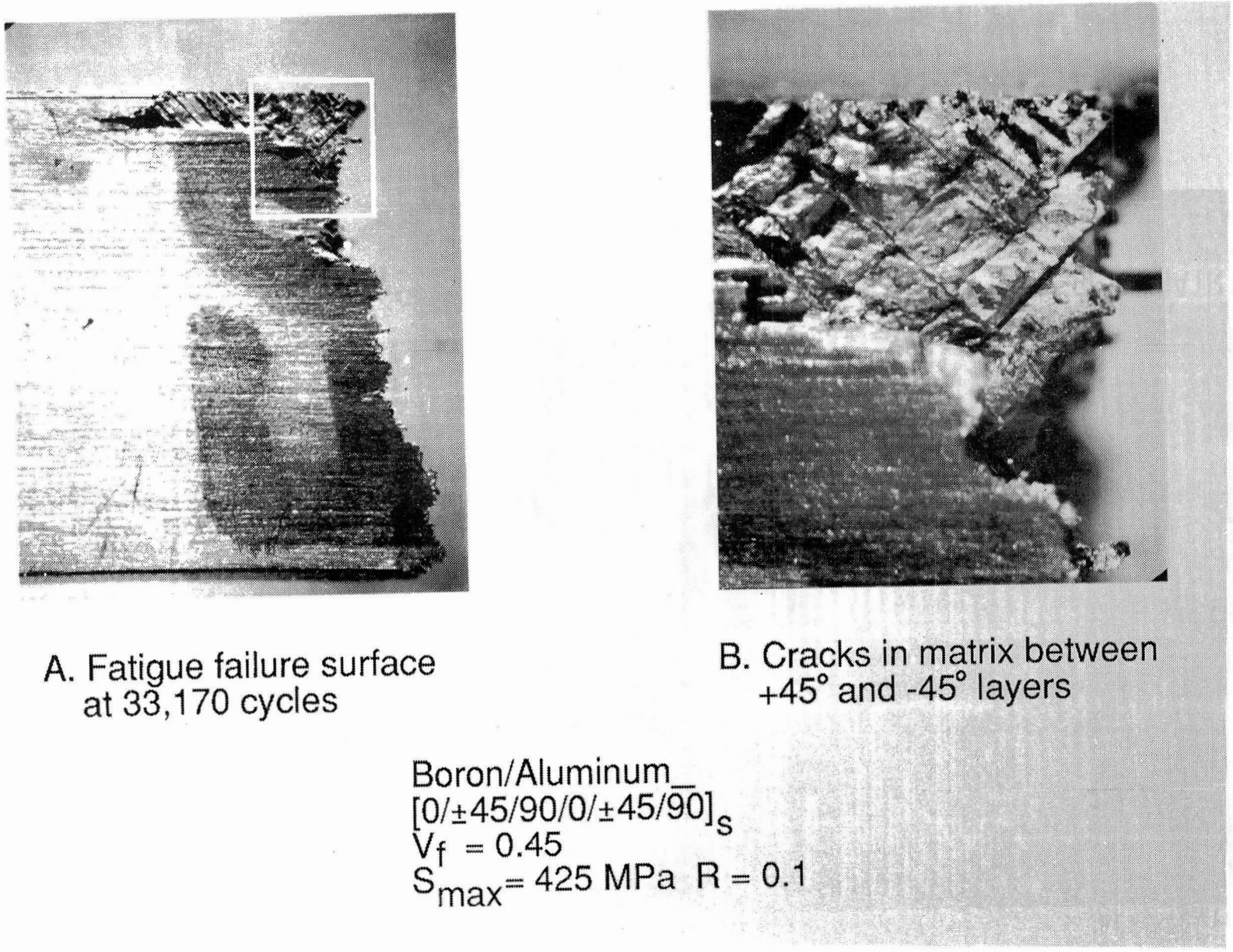

Fugure 8 - Cracks in the matrix between the +45° and -45° layers [2].

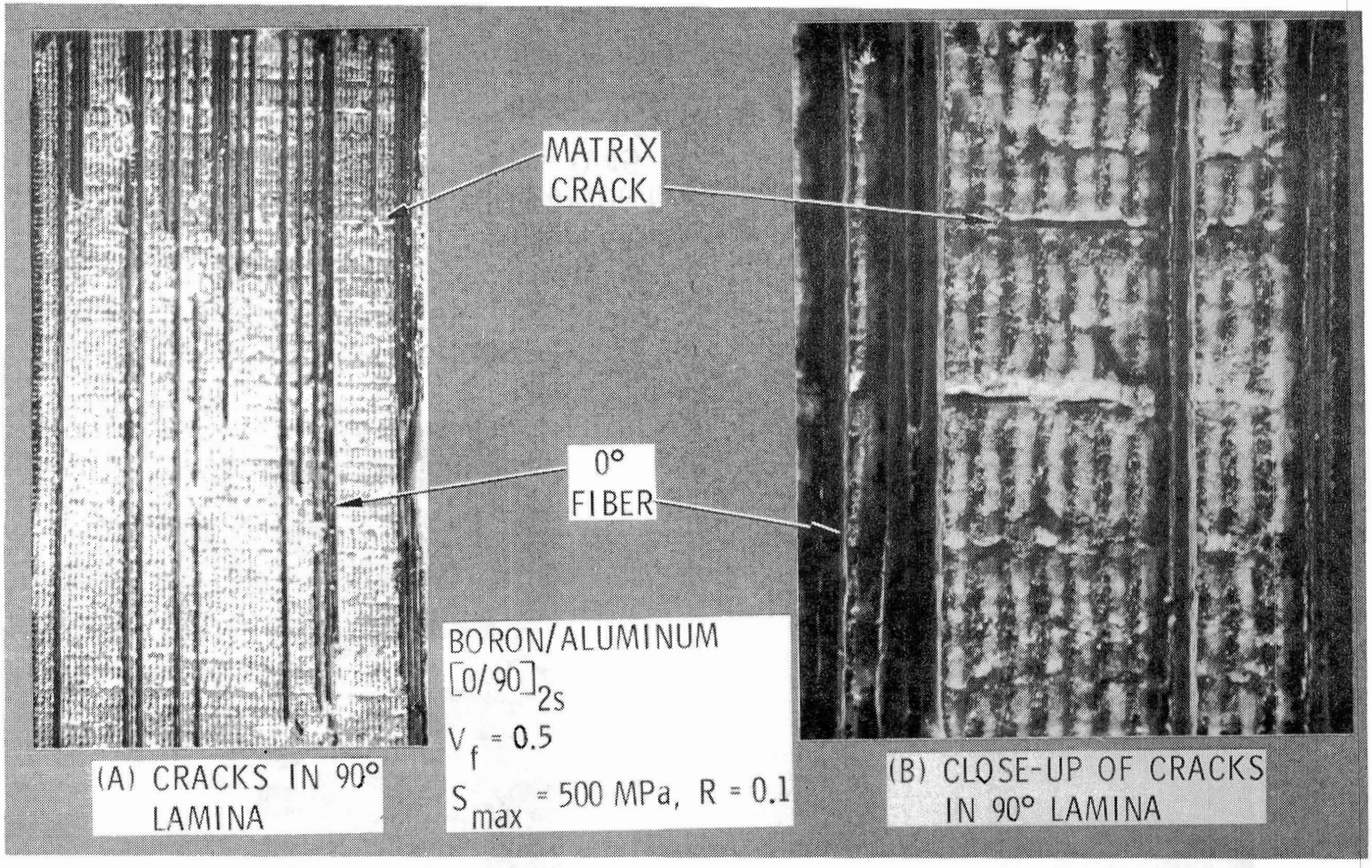

Figure 9 - Matrix cracks in the 90° lamina as exposed by etching away the 0° matrix material [3].

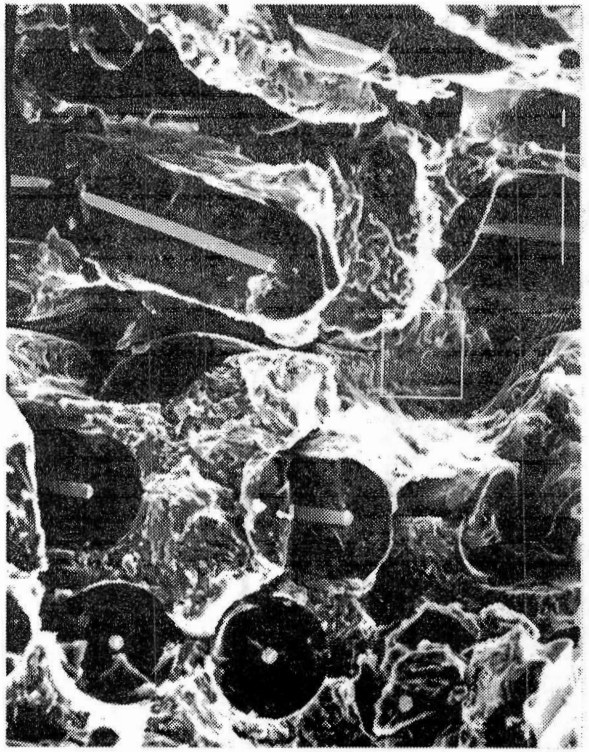

A. Fatigue failure surface
at 1,187,760 cycles

B. Fatigue striations in
-45° direction

Boron/Aluminum
$[0/\pm45/90/0/\pm45/90]_s$
$V_f = 0.45$
$S_{max} = 350$ MPa $R = 0.1$

Figure 10 - Evidence of fatigue crack propagation [1].

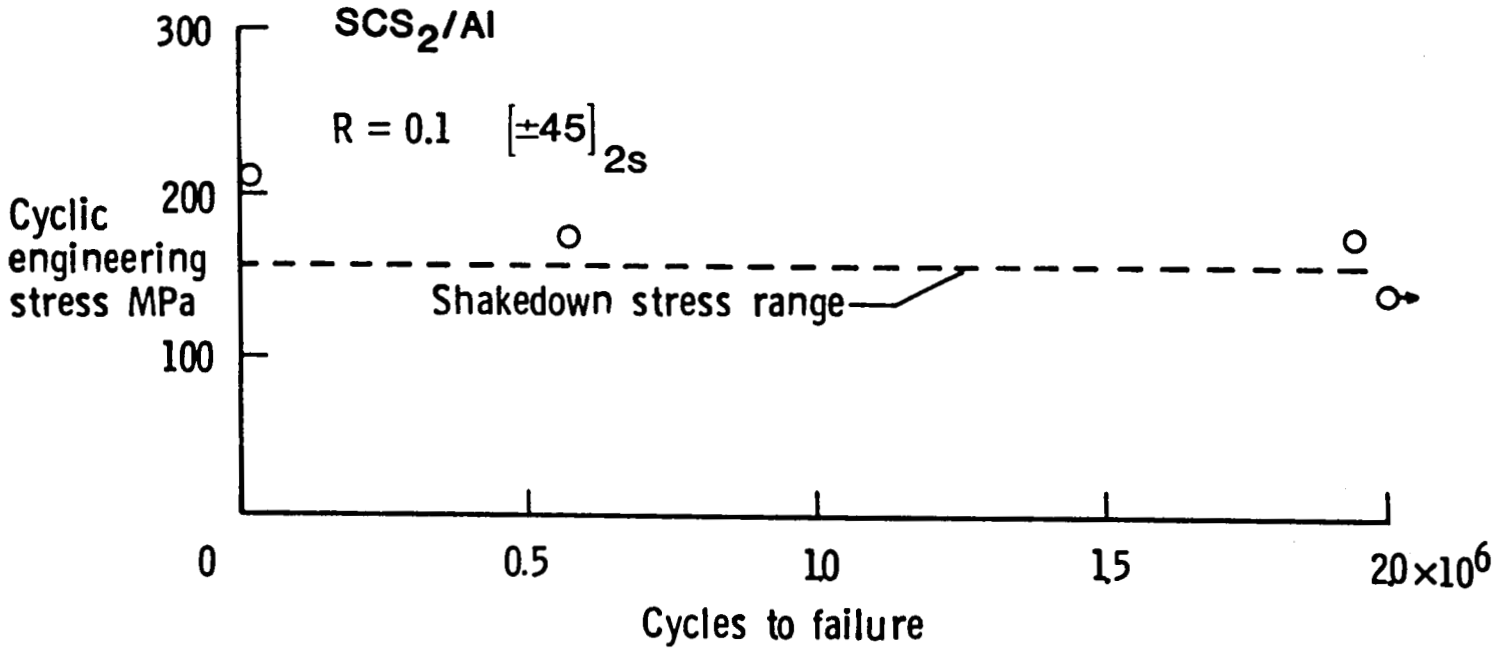

Figure 11 - S-N Curve [5].

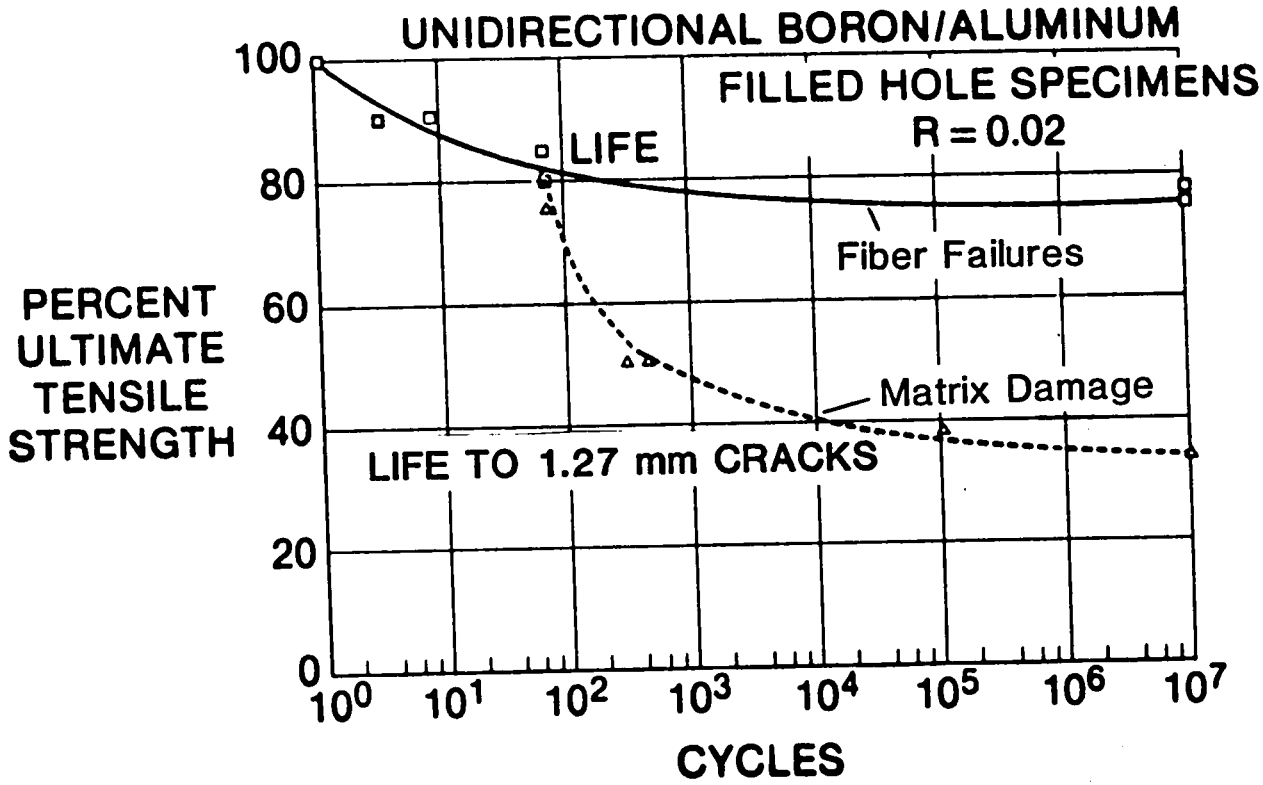

Figure 12 - Matrix cracking and fiber failure curves in B/Al unidirectional specimen containing a filled hole [17].

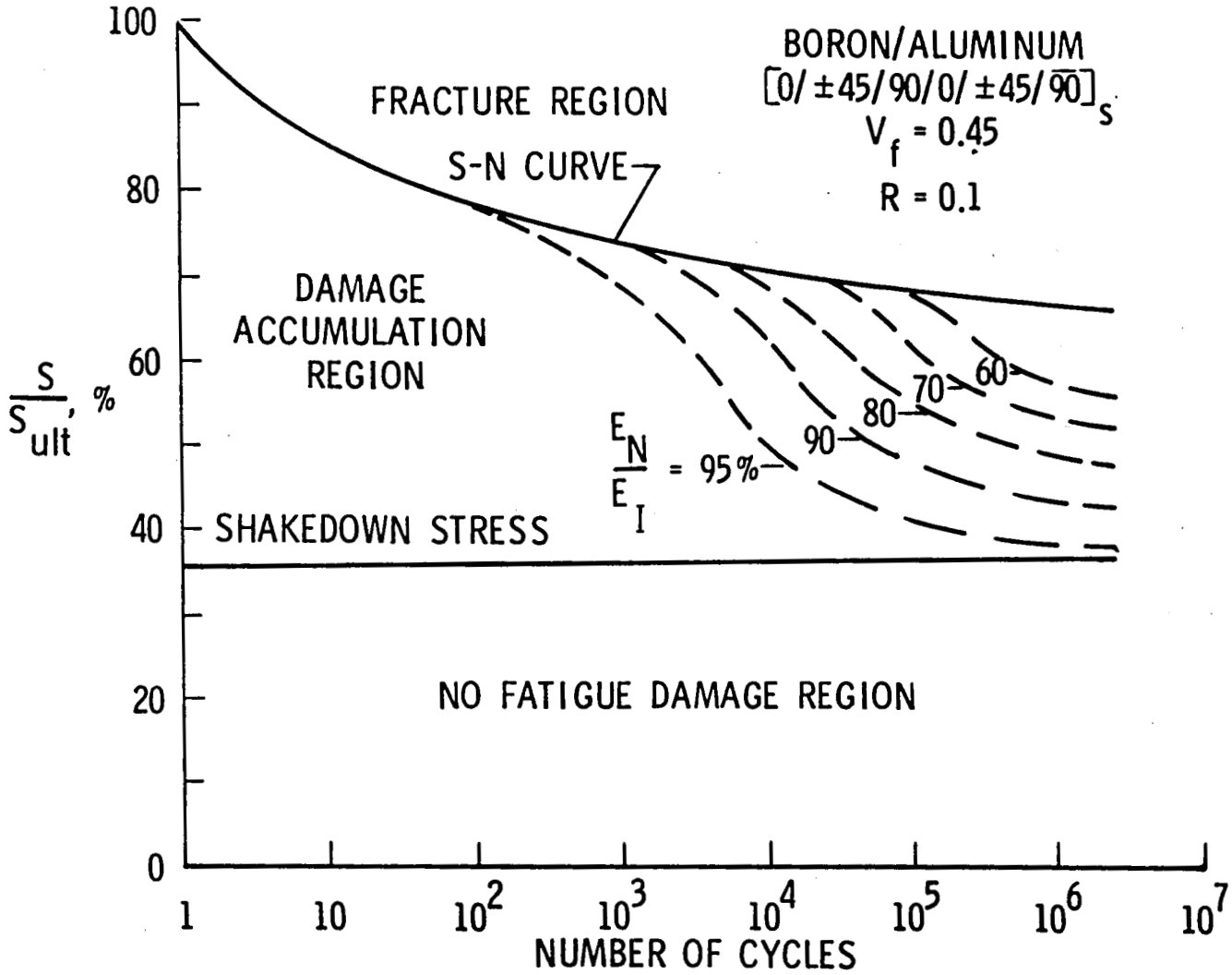

Figure 13 - Three regions of response to fatigue loading [10].

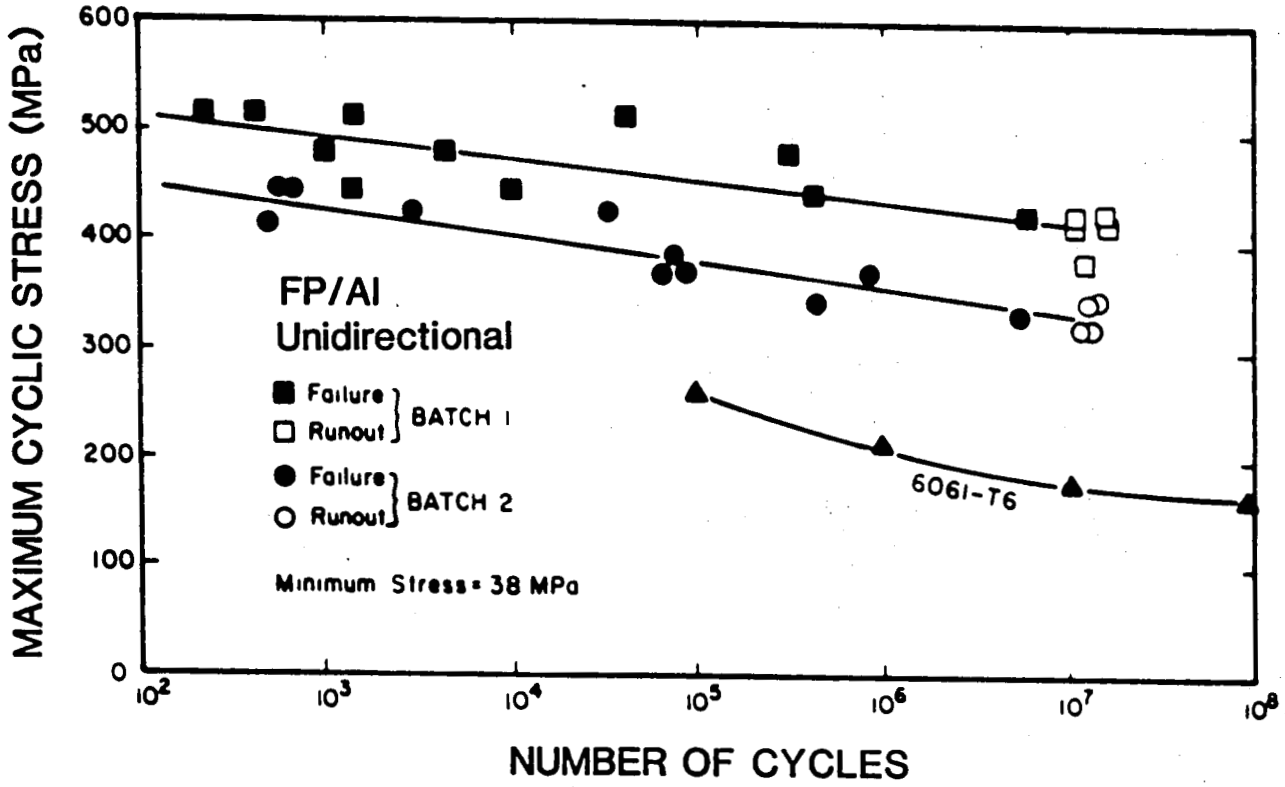

Figure 14 - S-N curves for unidirectional FP/Al. Fiber volume fraction was 55% [19].

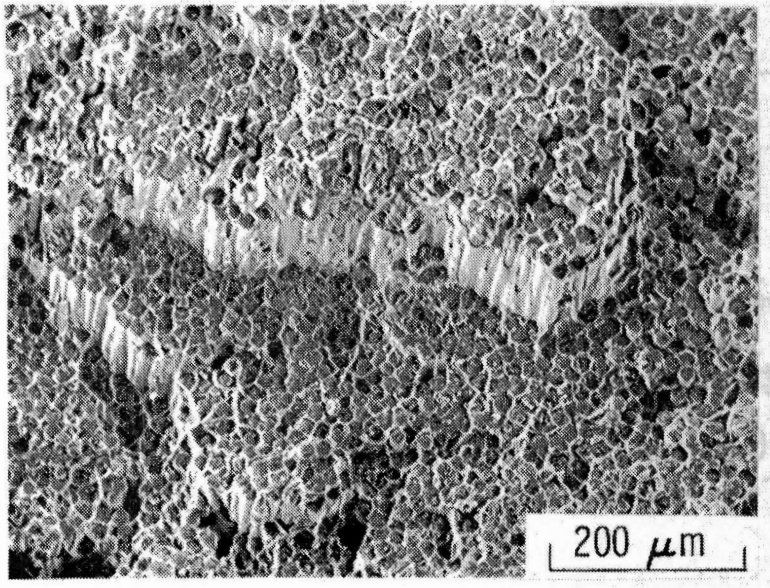

Figure 15 - Typical fracture surface topography for unidirectional FP/Al [19].

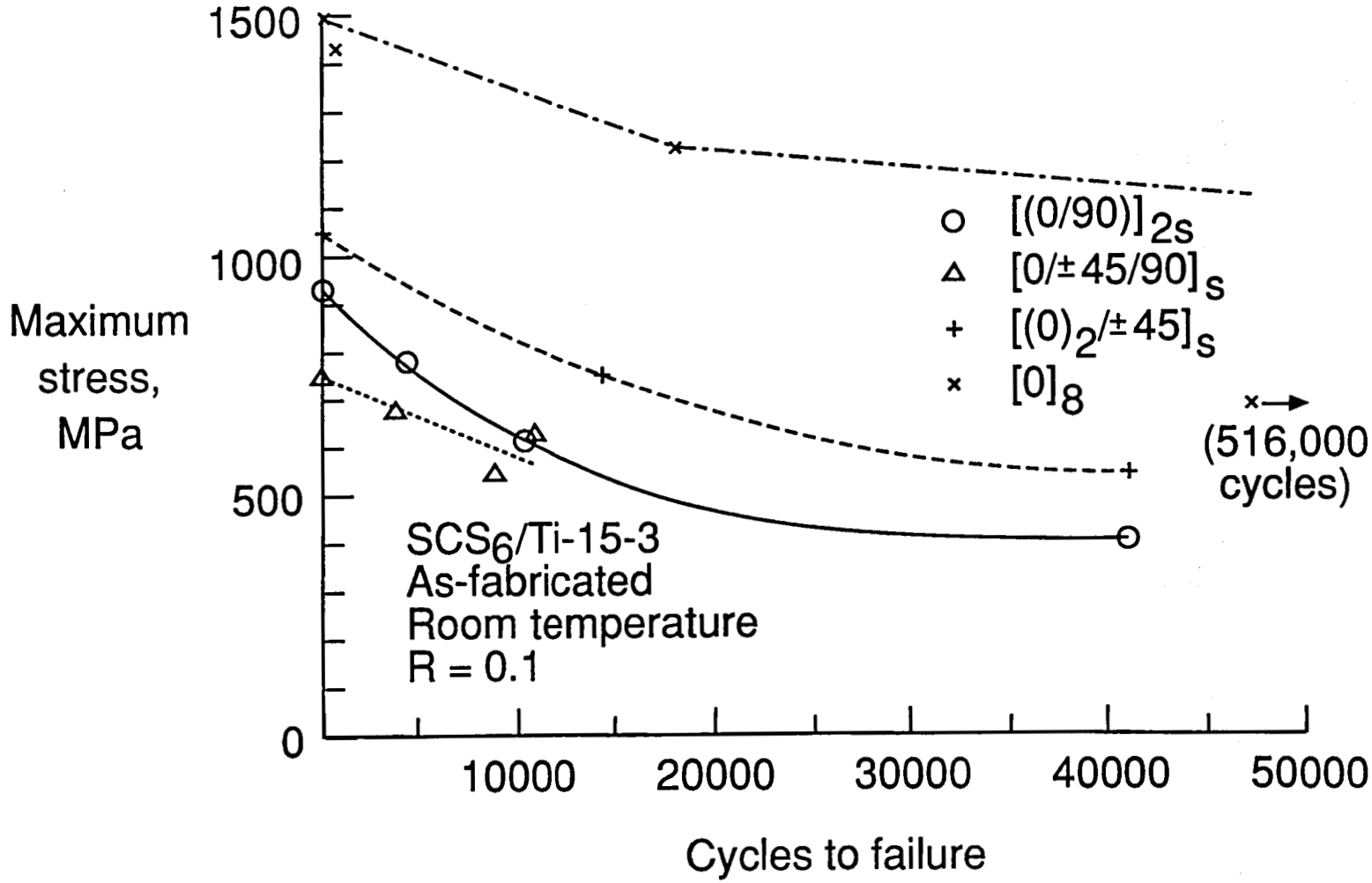

Figure 16 - S-N curves for SCS_6/Ti-15-3 laminates containing 0° plies.

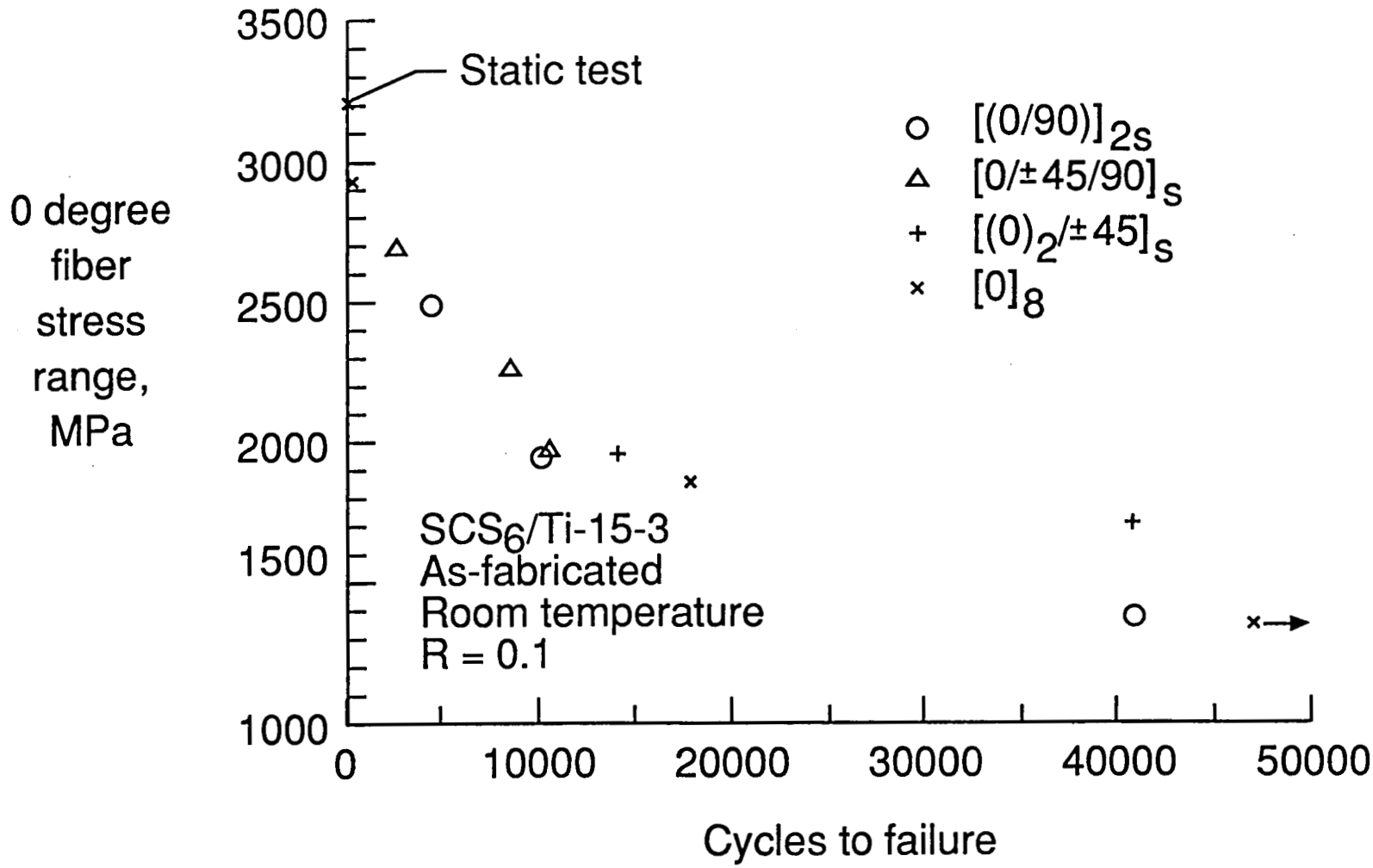

Figure 17 - Cyclic stress range in 0° fiber versus number of cycles to laminate failure.

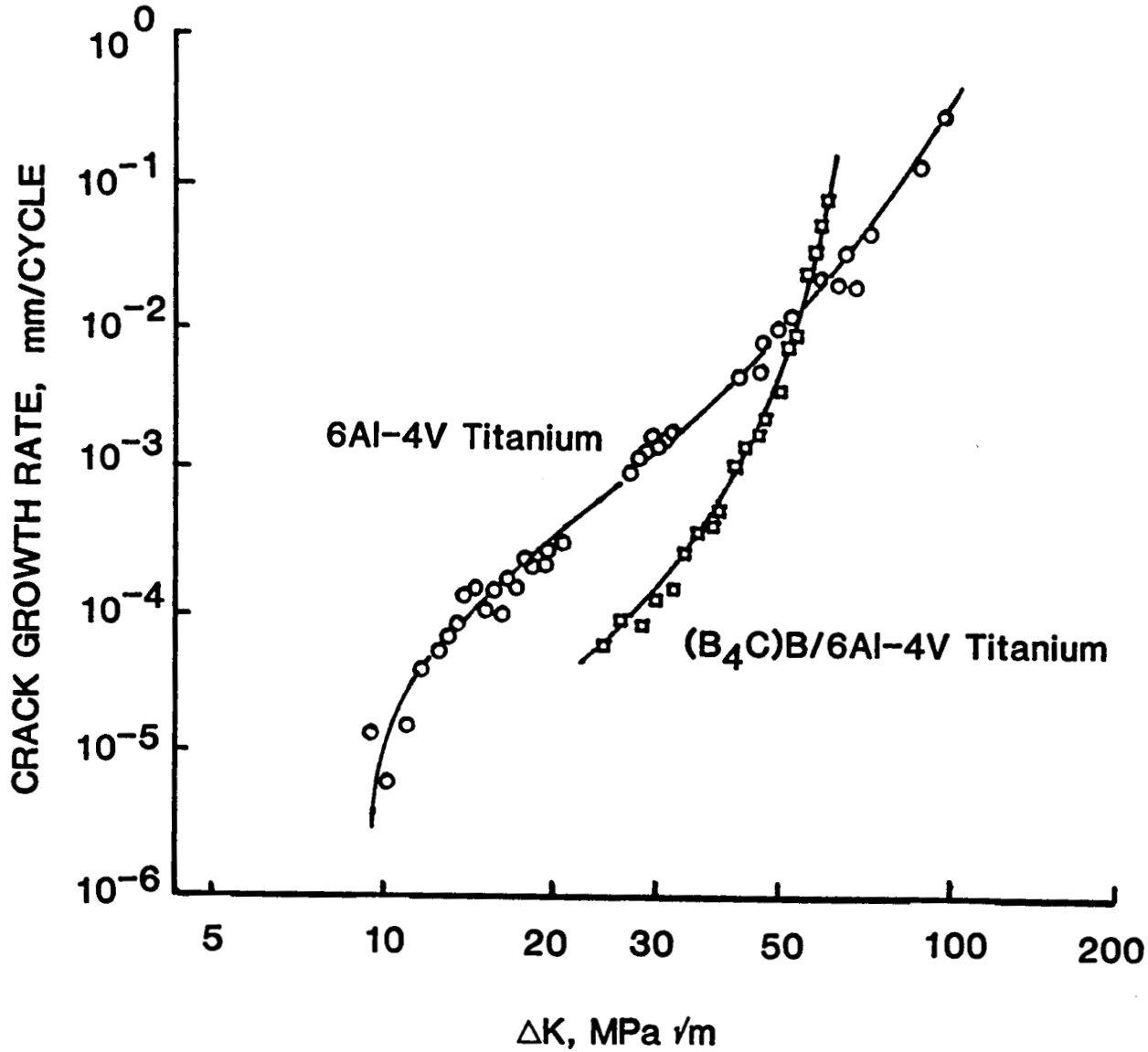

Figure 18 - Crack growth in titanium with and without unidirectional fiber reinforcement [17].

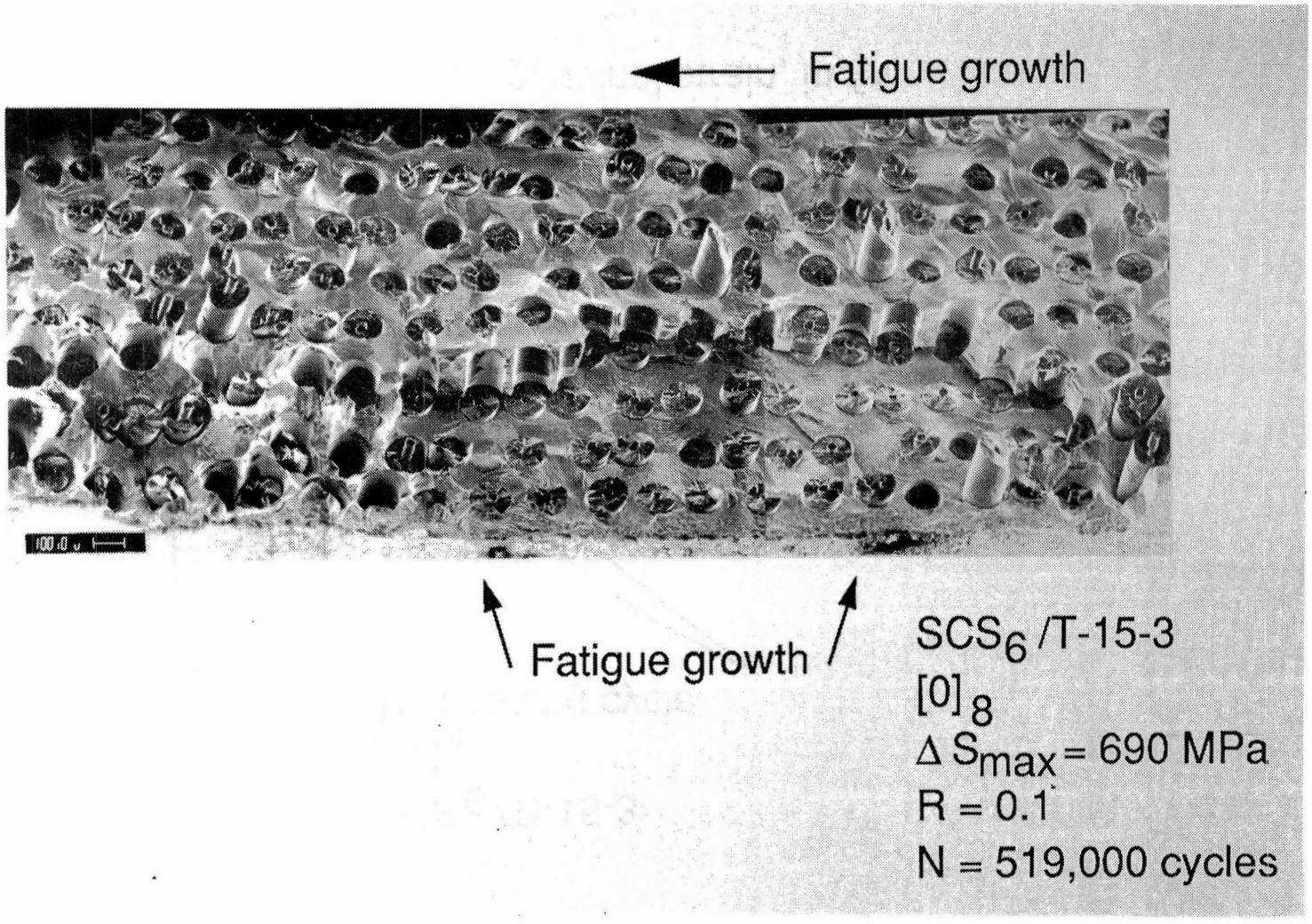

Figure 19 - Micrograph of the intersection of two fatigue cracks that have grown in a self-similar fashion.

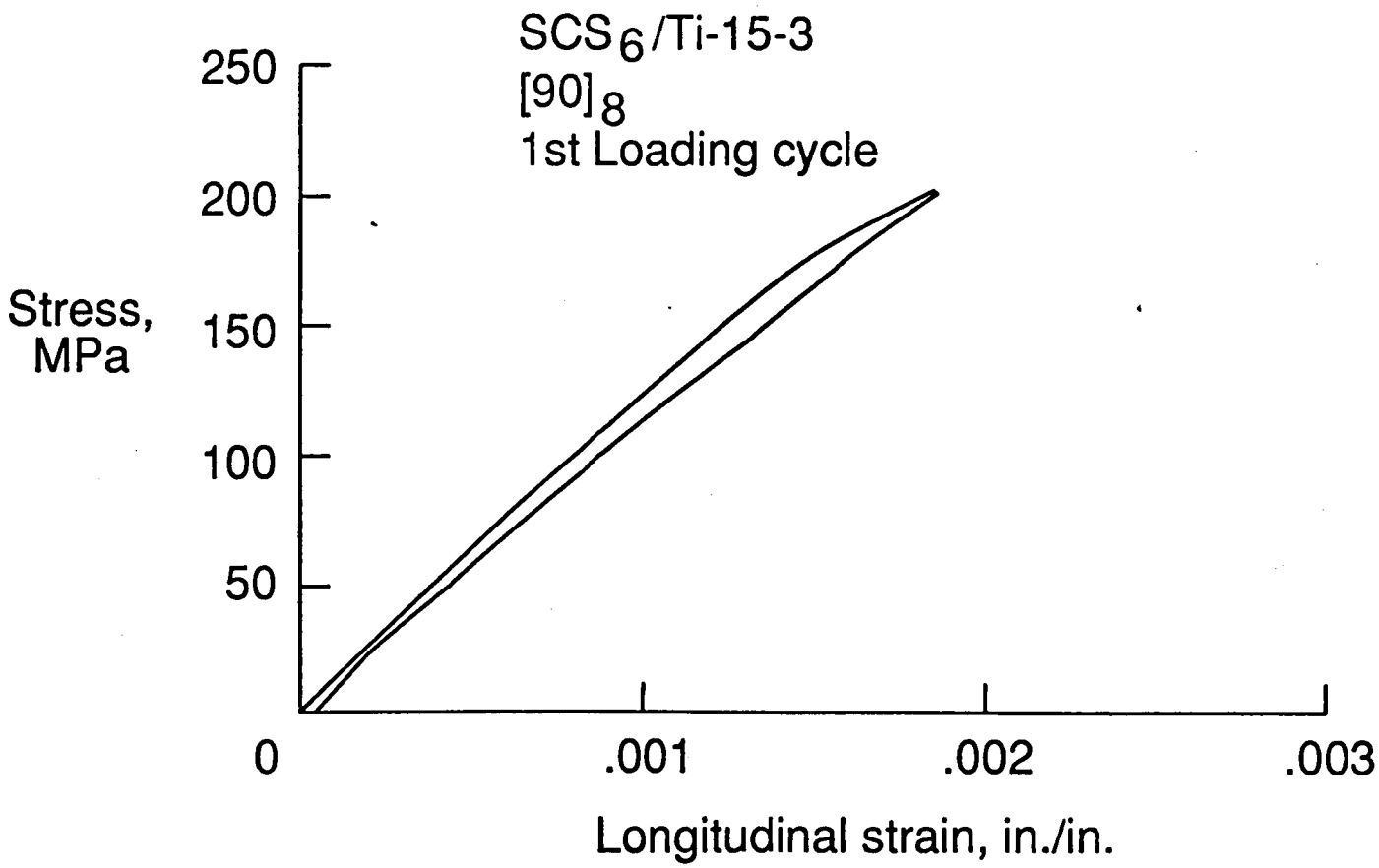

Figure 20 - Initial stress-strain response [24].

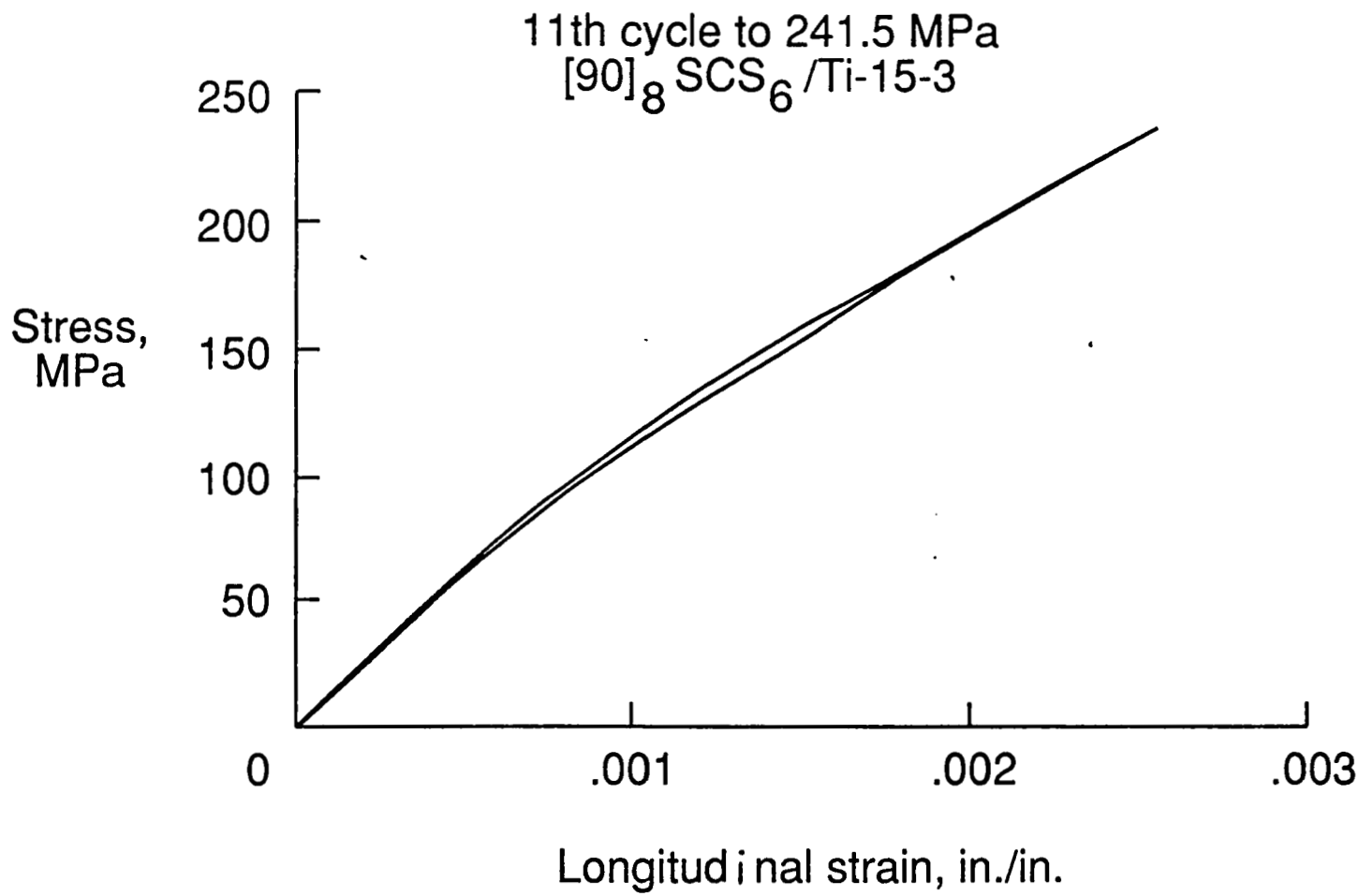

Figure 21 - The stress-strain response of the 11th applied cycle. (Typical response after the first applied cycle) [24].

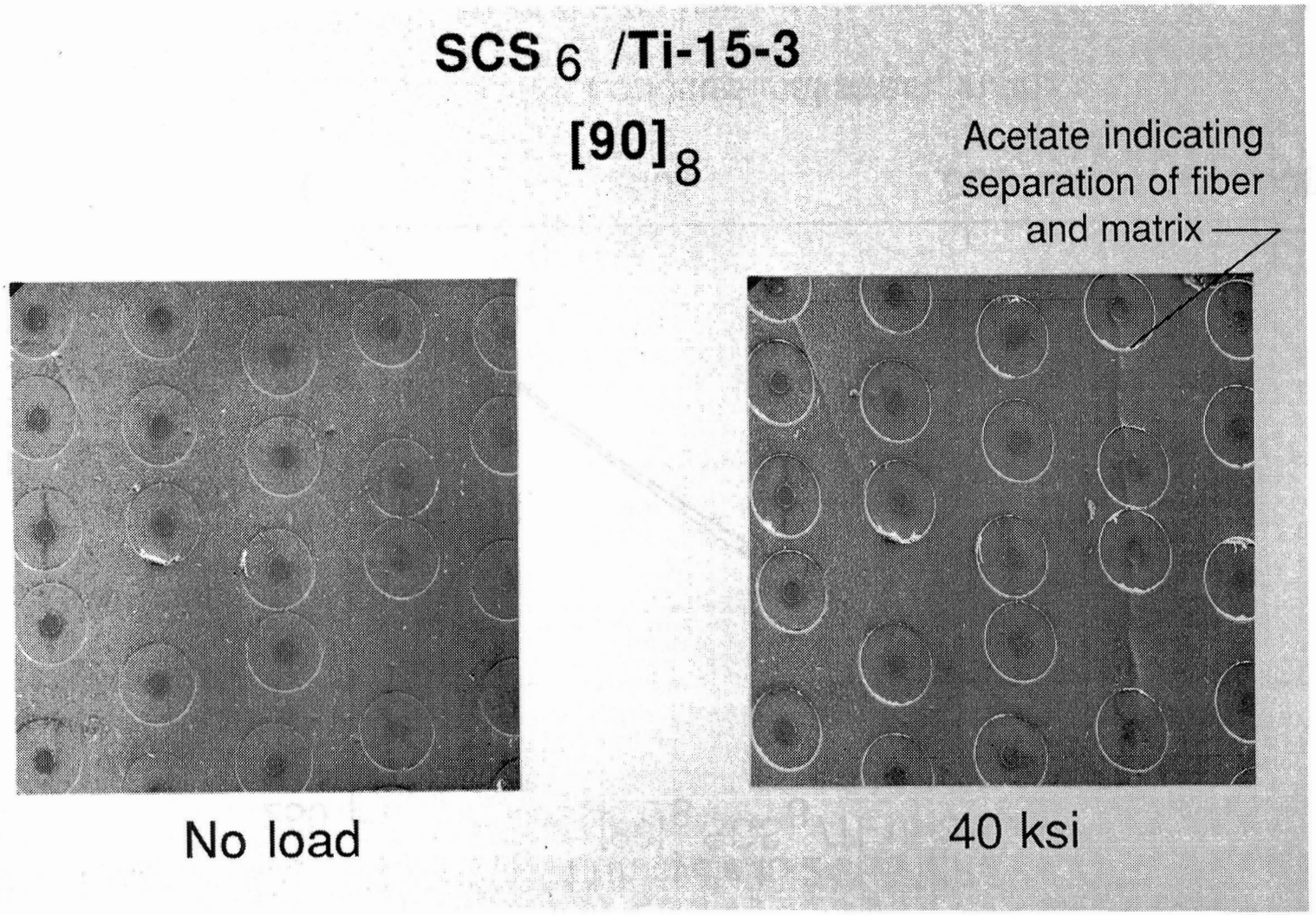

Figure 22 - Edge replicas of $[90]_8$ specimen. Note gaps between fiber and matrix at 414 MPa but not at NO load [24].

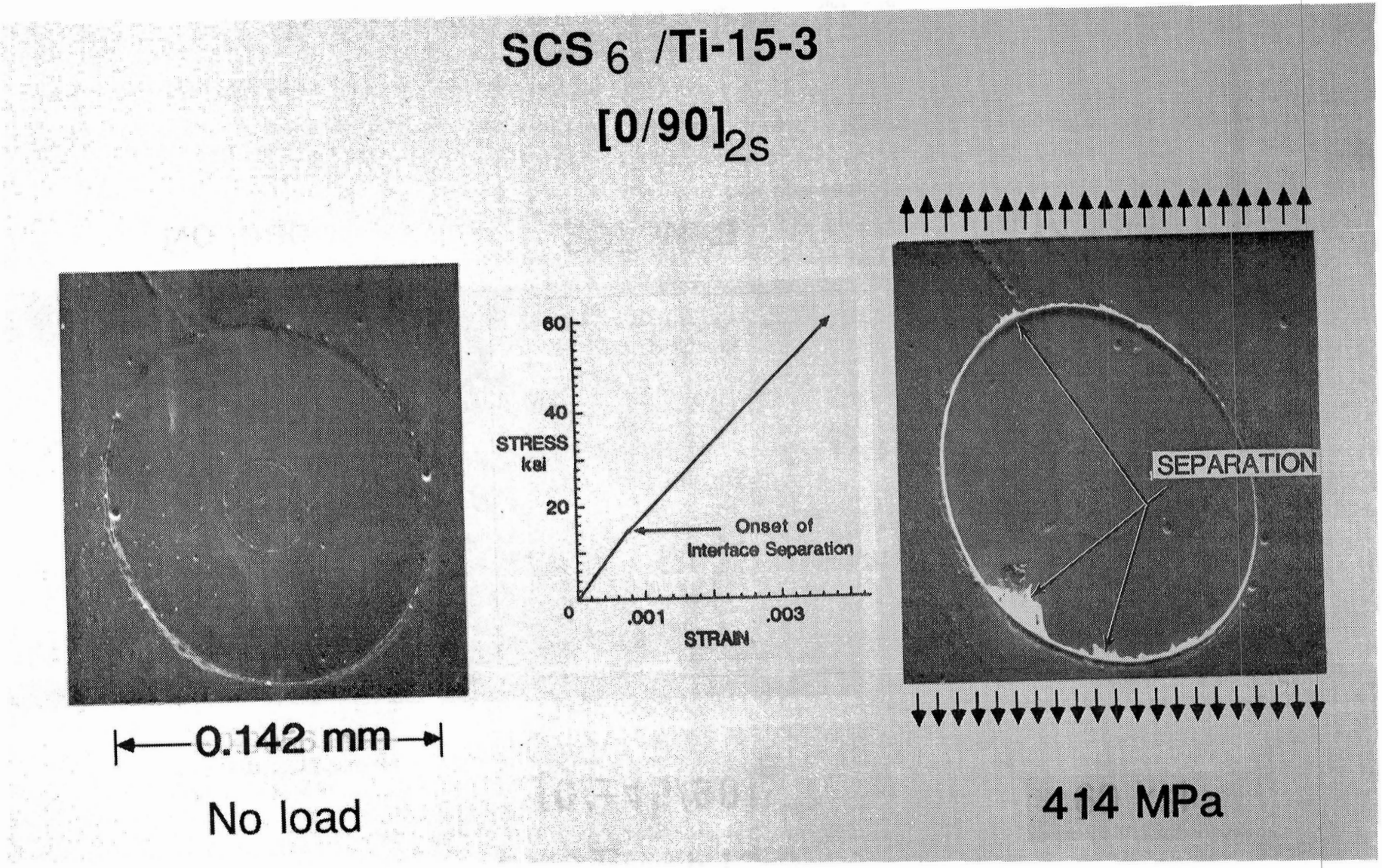

Figure 23 - Edge replicas of a 90° lamina fiber under laod and NO load [24].

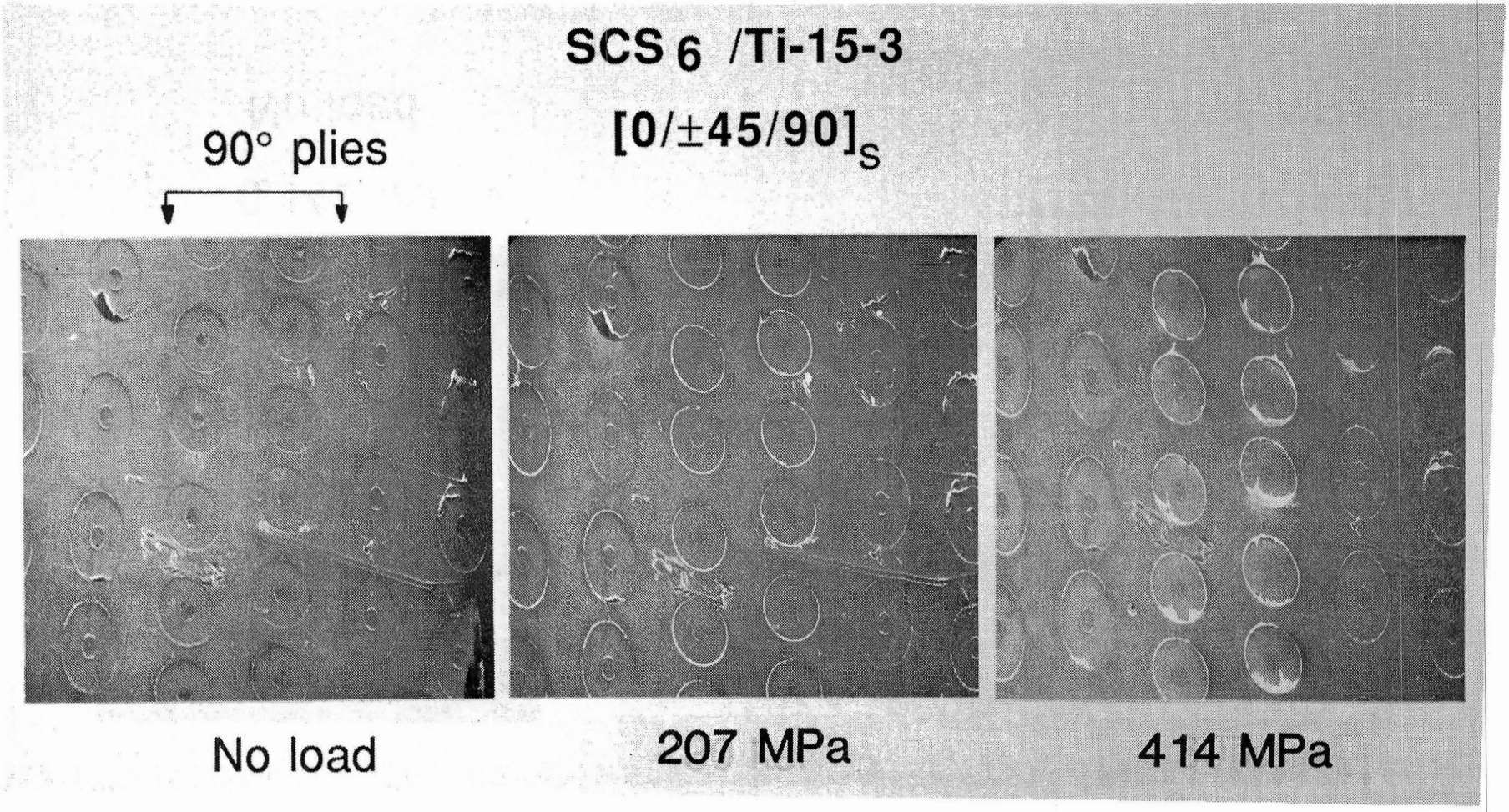

Figure 24 - Edge replicas of a $[0/\pm45/90]_s$ laminate.
90° plies are in the center of each photo [24].

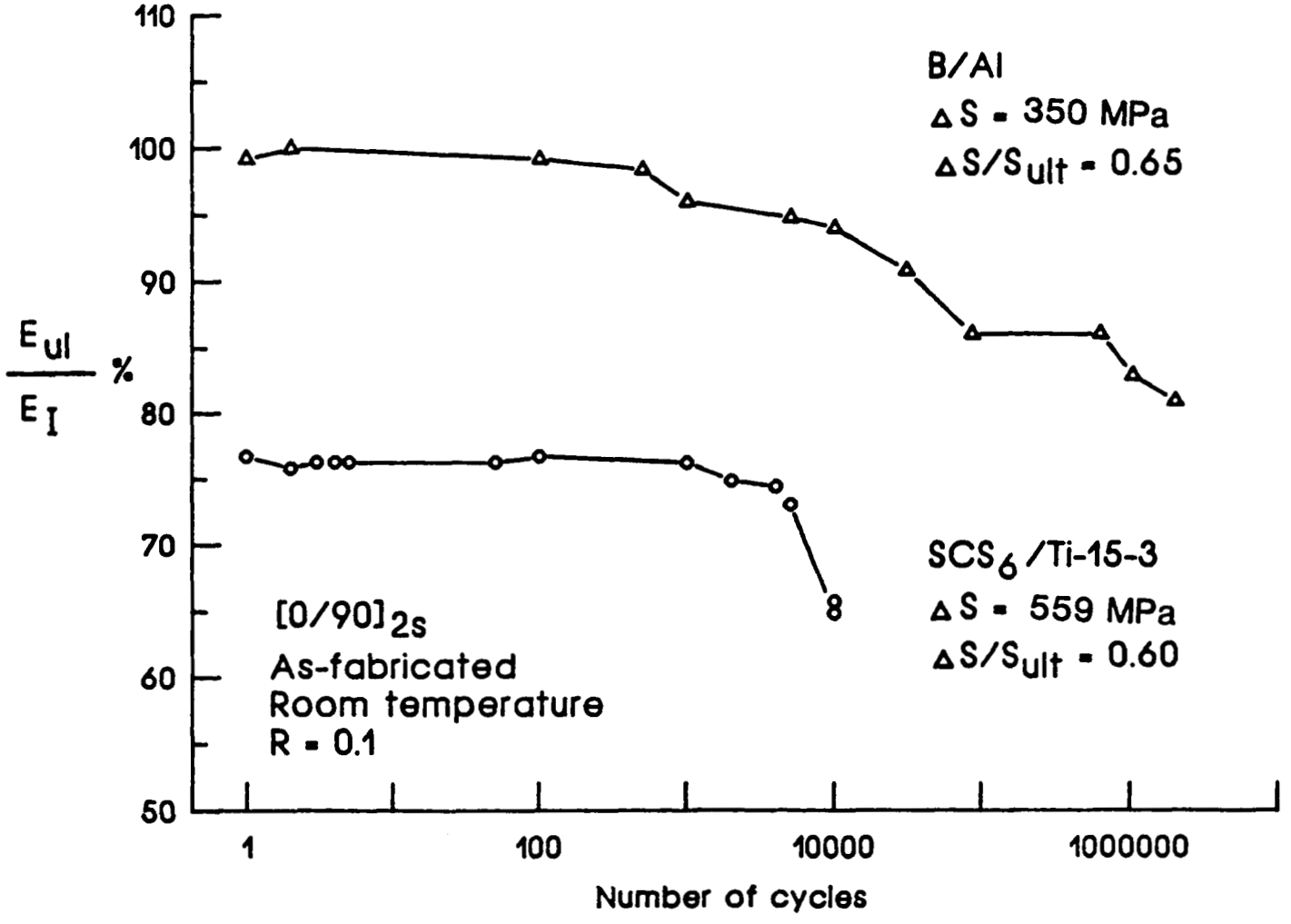

Figure 25 - Change in the elastic unloading modulus for $[0/90]_{2s}$ layups of B/Al and SCS_6/Ti-15-3.

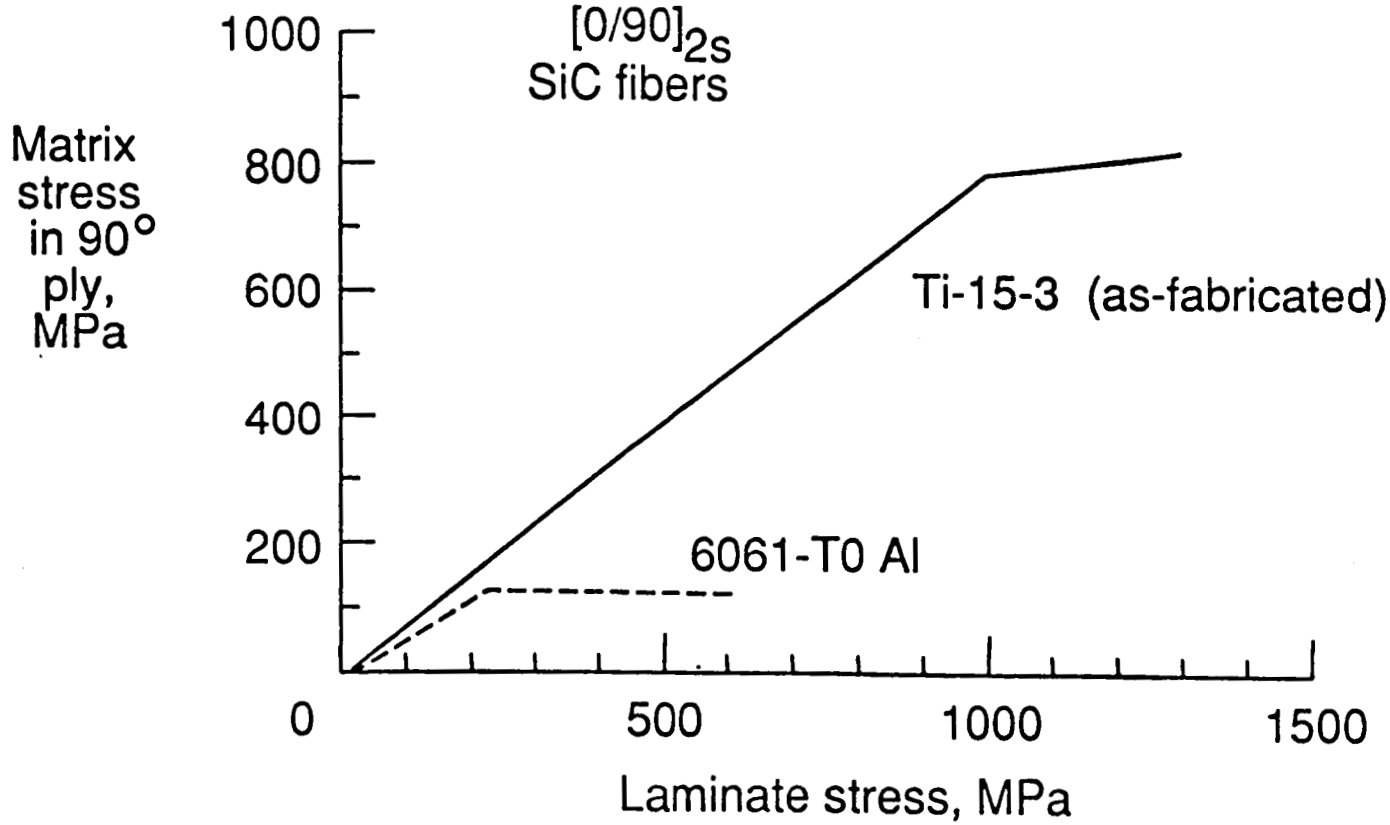

Figure 26 - Matrix stresses in the 90° plies of a $[0/90]_{2s}$ laminates [24].

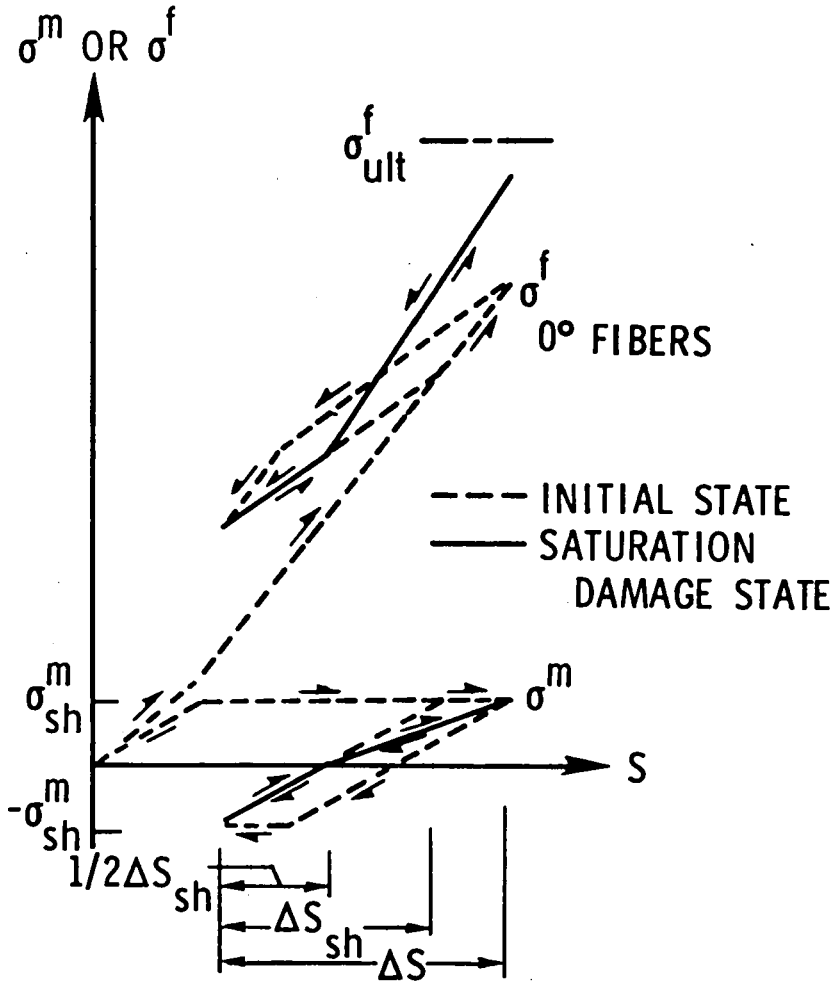

Figure 27 - Matrix and fiber stress response to applied laminate stress prior to and after the development of the saturation damage state [4].

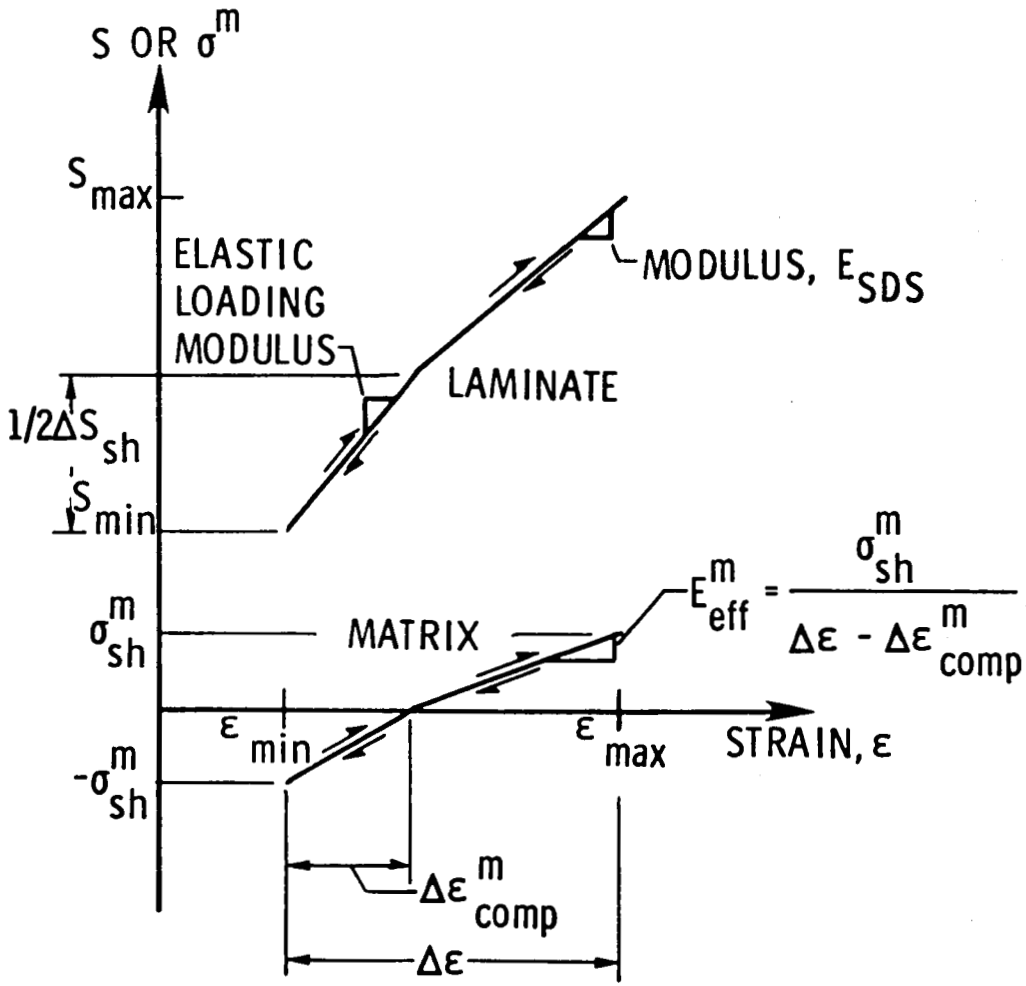

Figure 28 - Composite laminate and matrix stress-strain response for a saturation damage state [4].

NASA

Report Documentation Page

1. Report No.	2. Government Accession No.	3. Recipient's Catalog No.
NASA TM-100628		

4. Title and Subtitle	5. Report Date
FATIGUE TESTING AND DAMAGE DEVELOPMENT IN CONTINUOUS FIBER REINFORCED METAL MATRIX COMPOSITES	June 1988
	6. Performing Organization Code

7. Author(s)	8. Performing Organization Report No.
W. S. Johnson	
	10. Work Unit No. 505-63-01

9. Performing Organization Name and Address	11. Contract or Grant No.
National Aeronautics and Space Administration Langley Research Center Hampton, VA 23665-5225	
	13. Type of Report and Period Covered: Technical Memorandum
12. Sponsoring Agency Name and Address	
National Aeronautics and Space Administration Washington, DC 20546-0001	14. Sponsoring Agency Code

15. Supplementary Notes

16. Abstract

Continuous fiber reinforced metal matrix composites (MMC) are projected for use in high temperature, stiffness critical parts that will be subjected to cyclic loadings. This paper presents a general overview of the fatigue behavior of MMC. The objectives of this paper are twofold. The first objective is to present experimental procedures and techniques for conducting a meaningful fatigue test to detect and quantify fatigue damage in MMC. These techniques include interpretation of stress-strain responses, acid etching of the matrix, edge replicas of the specimen under load, radiography, and micrographs of the failure surfaces. In addition, the paper will show how stiffness loss in continuous fiber reinforced metal matrix composites can be a useful parameter for detecting fatigue damage initiation and accumulation. Second, numerous examples of how fatigue damage can initiate and grow in various MMC are given. Depending on the relative fatigue behavior of the fiber and matrix, and the interface properties, the failure modes of MMC can be grouped into four categories: (1) matrix dominated, (2) fiber dominated, (3) self-similar damage growth, and (4) fiber/matrix interfacial failures. These four types of damage will be discussed and illustrated by examples with the emphasis on the fatigue of unnotched laminates.

17. Key Words (Suggested by Author(s))	18. Distribution Statement
Metal matrix composites Aluminum Titanium Fatigue Matrix cracking Fiber/Matrix interface	Unclassified - Unlimited Subject Category 24

19. Security Classif. (of this report)	20. Security Classif. (of this page)	21. No. of pages	22. Price
Unclassified	Unclassified	53	A04